MOLECULAR SIMULATION STUDIES OF MDEA ABSORPTION PROCESS FOR CO_2 CAPTURE

SIN WAI KEAN

BACHELOR OF CHEMICAL ENGINEERING
UNIVERSITI MALAYSIA PAHANG

Thesis Access Form

No_____Location_____

Author: SIN WAI KEAN

Title : MOLECULAR SIMULATION STUDIES OF MDEA ABSORPTION PROCESS FOR CO2 CAPTURE

Status of access OPEN / RESTRICTED / CONFIDENTIAL

Moratorium period:_____ years, ending_____/_____200____

Conditions of access proved by (CAPITALS): DR NOORLISA BINTI HARUN

Supervisor (Signature)……

Faculty: Faculty of Chemical & Natural Resources Engineering

Author's Declaration: *I agree the following conditions:*

OPEN access work shall be made available in the University Malaysia Pahang only and not allowed to reproduce for any purposes.

*The statement itself shall apply to **ALL** copies:*

This copy has been supplied on the understanding that it is copyright material and that no quotation from the thesis may be published without proper acknowledgement.

Restricted/confidential work: All access and any photocopying shall be strictly subject to written permission from the University Head of Department and any external sponsor, if any.

Author's signature…….Date: ……

users declaration: for signature during any Moratorium period (Not Open work): ***I undertake to uphold the above conditions:***			
Date	Name (CAPITALS)	Signature	Address

MOLECULAR SIMULATION STUDIES OF MDEA ABSORPTION PROCESS FOR CO_2 CAPTURE

SIN WAI KEAN

Thesis submitted in partial fulfilment of the requirements
for the award of the degree of
Bachelor of Chemical Engineering

Faculty of Chemical & Natural Resources Engineering
UNIVERSITI MALAYSIA PAHANG

JANUARY 2015

SUPERVISOR'S DECLARATION

We hereby declare that we have checked this thesis and in our opinion, this thesis is adequate in terms of scope and quality for the award of the degree of Bachelor of Chemical Engineering.

Signature :
Name of main supervisor : DR. NOORLISA BINTI HARUN
Position : SENIOR LECTURER
Date :

STUDENT'S DECLARATION

I hereby declare that the work in this thesis is my own except for quotations and summaries which have been duly acknowledged. The thesis has not been accepted for any degree and is not concurrently submitted for award of other degree.

Signature :
Name : SIN WAI KEAN
ID Number : KA11117
Date : JANUARY 2015

Dedication

I dedicate my dissertation work to my family and all friends. Throughout my life two persons have always been there when I am facing any difficulty and frustration. I would like to dedicate this thesis and everything I do to my loving parents, Sin Yew Fook and Khong Kam Mooi whose give the words of encouragement and push for tenacity ring in my ears. Both of you have been my best cheerleaders. Next, I want to dedicate this dissertation to Kakak Emyra and Kakak Hana for helping me a lot in using and develop molecular dynamic simulations. Besides that, Kakak Hana will also share her knowledge on how to interpret and analysis the results from the simulations. Last but not least, I would like to thank Dr. Noorlisa binti Harun for her guidance and precious experience on how to write a good thesis.

ACKNOWLEDGEMENT

I would like to thanks the following people and organisations;

- My supervisors Dr. Noorlisa binti Harun and Kakak Emyra for their guidance through an effective well-arranged weekly meeting.
- Meanwhile, thanks to Kakak Hana for the guidance of simulating the molecules (MDEA, H_2O and CO_2) using Material Studio Software Package 6.1.

ABSTRACT

Concentration of CO_2 in the earth is gradually increasing every year due to the increased energy use by an expanding economy and population, and an overall growth in emissions come from electricity generation and transportation. Since CO_2 is a greenhouse gas, it will trap the heat inside the earth from reflecting back to the outer space and consequently contribute to global warming. So, methyldiethanolamine (MDEA) absorption for CO_2 capture process is developed to combat this trend due to its relatively high capacity, a low vapor pressure and small enthalpy of reaction with acid gases. Therefore, a research of studying methyldiethanolamine (MDEA) absorption process for CO_2 capture through simulation is developed so that the intermolecular interaction between the solvent (MDEA) and the acid gas (CO_2) during the absorption process can be investigated. Through the simulation, the optimum temperature of the carbon dioxide absorption will be determined. Molecular dynamic (MD) simulation will be used to study the interaction of molecule and give an insight on CO_2 absorption process. To perform the molecular dynamic (MD) simulation two boxes of carbon dioxide gas and MDEA solvent will combine to study the absorption process. Moreover, thermodynamic condition under NVE, NPT and NVT will be set and the simulation results will be interpreted in terms of radical distribution function. Mean square displacement (MSD) is then used to determine the diffusivity of molecules. MD simulation is performed at temperature of 40°C and 45°C to observe the potential interaction of molecules. Binary system studies the solubility of MDEA in water. Tertiary system studies the potential interaction of CO_2 in MDEA solution. It can be concluded that the molecular dynamic simulation clearly shows the potential interaction of molecules and its behaviour.

ABSTRAK

Kepekatan CO_2 di bumi meningkat secara beransur-ansur setiap tahun disebabkan peningkatan penggunaan tenaga oleh ekonomi dan penduduk yang berkembang, dan pertumbuhan keseluruhan dalam pengeluaran daripada penjanaan elektrik dan pengangkutan. Oleh sebab CO_2 ialah gas rumah hijau, ia akan memerangkap haba yang di dalam bumi daripada dicerminkan kembali ke angkasa lepas dan seterusnya menyumbang kepada pemanasan global. Jadi, proses penyerapan melalui methyldiethanolamine (MDEA) untuk menangkap CO_2 melalui simulasi dibangunkan untuk memerangi trend ini disebabkan kapasiti yang agak tinggi, tekanan wap yang rendah dan entalpi tindak balas dengan gas asid yang kecil. Oleh itu, satu penyelidikan tentang proses penyerapan melalui methyldiethanolamine (MDEA) untuk menangkap CO_2 melalui simulasi dibangunkan supaya interaksi antara molekul antara pelarut (MDEA) dan gas asid (CO_2) semasa proses penyerapan boleh difahami. Melalui simulasi, suhu optimum bagi penyerapan karbon dioksida akan ditentukan. Simulasi dinamik molekul (MD) akan digunakan untuk mengkaji interaksi antara molekul dan memberi gambaran mengenai proses penyerapan CO_2. Untuk melaksanakan simulasi dinamik molekul (MD) dua kotak gas karbon dioksida dan pelarut MDEA akan bergabung untuk mengkaji proses penyerapan. Selain itu, keadaan termodinamik di bawah NVE, NPT dan NVT akan ditetapkan dan keputusan simulasi akan ditafsirkan dari segi fungsi taburan yang radikal. Mean square displacement (MSD) kemudiannya digunakan untuk menentukan kemeresapan molekul. Simulasi MD dilakukan pada suhu 40°C dan 45°C untuk memerhati interaksi potensi molekul. Sistem binari mengkaji keterlarutan MDEA dalam air. Sistem ketiga mengkaji interaksi potensi CO_2 dalam MDEA. Ia boleh disimpulkan bahawa simulasi dinamik molekul jelas menunjukkan interaksi potensi molekul dan kelakuannya.

TABLE OF CONTENTS

LIST OF FIGURES

LIST OF TABLES

LIST OF ABBREVIATIONS

a_i	Acceleration
ε_o	Vacuum permittivity
ε_T	Relative permittivity
f_i	Force of Newton's second law of motion
m_i	Mass of particle
ρ	Density of atoms
r	Spherical radius
r_i	Change in particle position
$V(r_i)$	Potential energy respect to particle position
t	Time
∇_i	3 dimensions
Φ	Harmonic interaction force
Ψ_{nlm_l}	Wave function

Greek

Å	Angstrom
E	Energy
K	Harmonic force constant
M	Diffusion coefficient
N	Number of mole
N_i	atomic population
P	Pressure
P_{ii}	density matrix
S_{ii}	overlap matrix
T	Temperature
U_{AB}	Potential Energy
V	Volume

LIST OF ABBREVIATIONS

AO	Atomic orbitals
COMPASS	Condensed-phase optimized molecular potentials for atomic simulation studies
DEA	Diethanolamine
LJ	Lennard-Jones potential
LPA	Löwdin population analysis
MEA	Monoethanolamine
MD	Molecular dynamics simulation
MDEA	Methyldiethanolamine
MM	Molecular mechanic
MO	Molecular wave functions
MPA	Mulliken population analysis
MSD	Mean square displacement
NPT	Constant number of moles, pressures and temperatures
NVE	Constant number of moles, volumes and energies
NVT	Constant number of moles, volumes and temperatures
PBC	Periodic boundary condition (PBC)
QM	Quantum mechanic
RDF	radial distribution function

1 INTRODUCTION

1.1 Motivation and statement of problem

Nowadays, the issue of CO_2 emissions becomes more serious due to the increased energy use by an expanding economy and population, and an overall growth in emissions from electricity generation and transportation. All these human activities are altering the carbon cycle by adding more CO_2 to the atmosphere and by influencing the ability of natural sinks, like forests, to remove CO_2 from the atmosphere. This phenomenon causes the trapping of CO_2 inside the earth to increase drastically for past few decades (Rubin & De Coninck, 2005).

The CO_2 emissions bring bad effect to human beings and also environment too. Global warming caused by the trapping of CO_2 in the earth melts the ice caps from north and south poles corresponding to the rise of sea level. Densely settled coastal plains would become uninhabitable with just a small rise in sea level. Warming would result in the increased of high cloud cover in winter, giving chemical reactions a platform in the atmosphere, which could result in depletion of the ozone layer. A warmer climate could change the weather systems of the earth, meaning there would be more droughts and floods, and more frequent and stronger storms. Diseases would be able to spread to areas which were previously too cold for them to survive in. As with the diseases, the range of plants and animals would change, with the net effect of most organisms moving towards the North and South Poles.

Figure 1-1 shows that a large quantity of CO_2 is released every year due the combustion of fossil fuel to produce energy. The CO_2 emissions from fossil fuel combustion are increasing drastically especially from year 1990 to 2010. There are a few of carbon dioxide separation technologies but the chemical absorption is the most effective for the removal of carbon dioxide. In this study, the chemical solution used for process of chemical absorption is amine solution. The reaction between CO_2 and amines will enhance the driving force for the separation even at low partial pressure of CO_2 (IEA org, 2013).

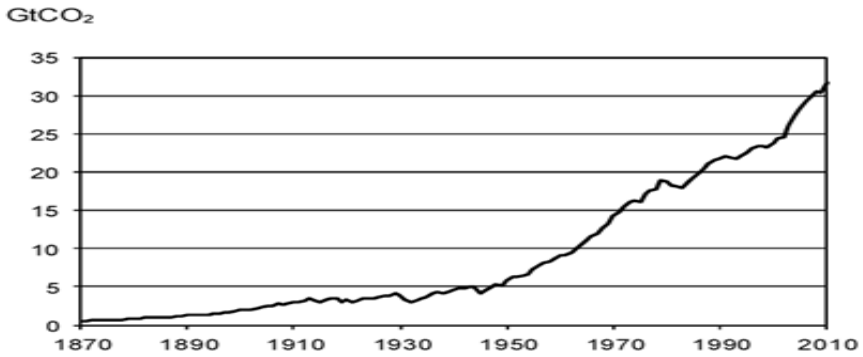

Figure 1-1: Trend in CO_2 emissions from fossil fuel combustion (IEA org, 2013)

Figure 1-2 shows that electricity and heat emits the highest total amount of CO_2 to the atmosphere compared to other sectors. Generation of electricity and heat worldwide relies heavily on coal, the most carbon-intensive fossil fuel. Countries such as Australia, China, India, Poland and South Africa produce over two-thirds of their electricity and heat through the combustion of coal. By 2035, the WEO 2013 projects that demand for electricity will be almost 70% higher than current demand, driven by rapid growth in population and income in developing countries, by the continuing increase in the number of electrical devices used in homes and commercial buildings, and by the growth in electrically driven industrial processes (IEA org, 2013).

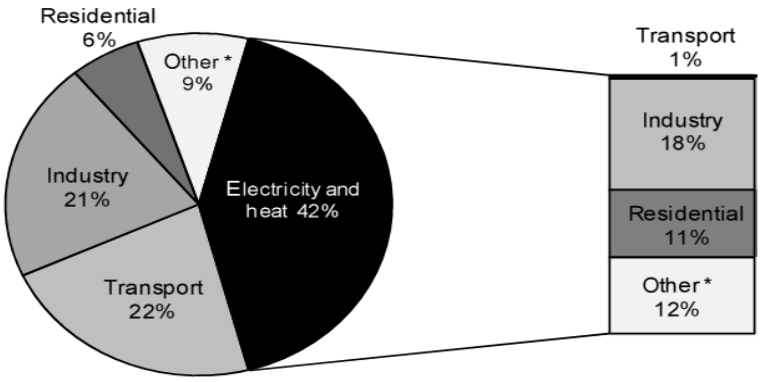

Figure 1-2: World CO_2 emissions by sector in 2011 (IEA org, 2013)

Therefore, the aim of this study is to understand the molecular level interaction during the process of CO_2 absorption using amine solution. The molecular dynamic simulation is used to simulate the molecular interaction of the absorption process. Through this simulation, the molecular interaction between amine solution and CO_2 can be understood better and can be applied to improve the performance of amine absorption

process. The outcome from this study can be used for future research on CO_2 capture to conserve and preserve our natural environment.

1.2 Objectives

This research project aims to:

- Study intermolecular interaction in methyldiethanolamine (MDEA) absorption for carbon dioxide capture via molecular dynamic simulation technique at different process operating conditions. The strength of intermolecular interaction between the CO_2 and the solvent will represent the absorption effectiveness.

1.3 Scope of this research

In this case study there are few scopes:

- Molecular Dynamic (MD) simulation is used to study and give insight on the intermolecular interaction between solvent and acid gases in the absorption process.
- There are different systems at various operating conditions are considered in this study; pure molecules (pure MDEA, pure water, and pure CO_2), binary system (MDEA+H_2O) and tertiary system (MDEA+CO_2+H_2O).
- The optimum molecular interaction will be determined by observing the highest intermolecular interaction between molecular while simulating the absorption process at different temperature.
- Mean square displacement is used to calculate the diffusion coefficient.

1.4 Main contribution of this work

This study gives insight on the molecular interaction between carbon dioxide and methyldiethanolamine (MDEA) during the absorption process. The maximum interaction during the absorption process will be determined at various process operating conditions. All the data in this simulation process can be used to contribute to the development of technologies for CO_2 removal.

1.5 Organisation of this thesis

The structure of the thesis is outlined as follow:

Chapter 2 reviews open literature of current thesis and introduces researches which have been conducted in this regard. There are some brief explanations on amine based absorption process for carbon dioxide and reactivity of alkanolamines. The interaction involved during the simulations and the thermodynamic properties used in this study are also clearly explained in this chapter.

Chapter 3 concerns the methodology used in this study. The procedure and forcefields involve in the simulation process. This chapter also explains the method to interpret radical distribution function into graphical form to analyse the interaction between atoms.

Chapter 4 discuss the results obtain from research and simulation carried out. The results will be related with the amine based absorption to give insight on how the interaction occur during the simulation and determine the optimum temperature of the absorption process.

Chapter 5 draws together a summary of the thesis and outlines the future work which might be derived from the model developed in this work.

2 LITERATURE REVIEW

2.1 Introduction

This chapter discusses carbon dioxide separation technologies, amine based absorption process, molecular dynamic simulation (MD) and modelling of molecules. The aim of this chapter is to review the fundamental science of the absorption process and the simulation technique.

2.2 Carbon dioxide separation technologies

Nowadays, there are many technologies available for gas separation especially CO_2 capture system. The known technologies are adsorption, membrane separation, cryogenic separation, physical and chemical absorption. The choice of a suitable technology depends upon the characteristics of the gas stream from which the CO_2 needs to be separated, the sensitivity of the method to other impurities or trace components, the amount of CO_2 recovery, the capital and operating costs and the environmental impacts (waste or by-product production) (Steeneveldt et al., 2006).

a) Adsorption

This technology is used for carbon dioxide removal from the flue gas using solid adsorbents. These solid adsorbents have a high surface area and desorb through a regeneration process. The adsorption process is typically cycled between two beds of adsorbents; one bed is adsorbing CO_2 while the other is being regenerated. In the regeneration process, CO_2 can be desorbed by either pressure swing adsorption (PSA) (pressure reduction) (Yokoyama, 2003), temperature swing adsorption (TSA) (temperature increase) (Drage et al., 2009), electrical swing adsorption (ESA) (Grande et al., 2009), which adjusts the electric current passed through the adsorbents, or vacuum swing adsorption (VSA) (Chaffee et al., 2007). PSA is commercially used for gas separation, in hydrogen production and in the removal of CO_2 from natural gas (Yong et al., 2002). However, the key challenge of CO_2 capture using adsorption technology is low capacity and selectivity for current adsorbents, which limits its application for large scale CO_2 removal.

b) Membrane separation

Application of membrane separation typically involves the use of polymer-based membranes employing permeation process. Form of membrane treatment includes spiral-wound system, tubular systems and hollow fiber. However, membrane is determined as not effective method because it cannot achieve high degrees of separation. It needs to have multiple stages and/or recycle of one of the streams is required. This will lead to increased energy consumption, cost and complexity. The advantages of a gas membrane separation process include lower capital cost, ease of skid-mounted installation, lower energy consumption, its ability to be installed in remote areas, especially offshore, and flexibility (IPCC, 2005).

The phenomenon of membrane separation occurs in 4 steps:

- Adsorption of the CO_2 by the active surface of the membrane (at the raw gas pressure)
- Dissolution of the CO_2 in the membrane
- Diffusion of the CO_2 through the membrane
- Desorption of the CO_2 from the membrane (at low pressure)

The adsorption of the CO_2 is better at high pressure (high CO_2 partial pressure). The process is then not well suited to low pressure operations. The polymeric material to be selected for membrane construction must be permeable to CO_2 but also selective (to avoid permeation of hydrocarbon gas components).

c) Cryogenic separation

The cryogenic separation is a process for the removal of CO_2 from natural gas. The process originally developed by KOCH Process Systems Inc. was titled "RYAN/HOLMES Process" after two employee-inventor and involves the use of a hydrocarbon additive usually present in the natural gas to provide a particular benefit to the distillation (lowering the CO_2 freezing point). The "RYAN/HOLMES Process" uses Natural Gas Liquid (NGL) which is extracted from the feed stream itself. (Maddox, 1982)

The principle of the "RYAN/HOLMES Process":

- Separation of methane from CO_2. This separation uses the NGL stream to avoid CO_2 freezing and takes place in the "RYAN/HOLMES demethanizer".

- Separation of CO_2 from ethane plus (C^{2+}). This separation uses the NGL stream to break the CO_2/ethane azeotrope.

Since this separation requires low temperature, its best utilization is the LNG manufacture. Derived cryogenic processes working at temperature above the CO_2 solidification point have been implemented for the bulk removal of CO_2 from natural gas.

d) Physical absorption

Physical absorption relates to the use of molecular sieves for the removal of acid gases. It uses organic or inorganic solvents to physically absorb the CO_2. This process is mostly applicable to gas streams which have relatively concentrated streams of CO_2 at high pressure. They are commercially used to remove acid gases, CO_2 and H_2S from natural gas for removing CO_2 from synthesis gas in ammonia, hydrogen, and methanol production. Some commercially available solvents include dimethyl ether, propylene carbonate, N-methyl-2-Pyrrolidone and methanol (Abass, 2010). For the process of physical adsorption, firstly the untreated gas is contacted with the solvent which absorbs CO_2 in an absorber column. Secondly, the CO_2 rich liquid stream exits the bottom of the absorber and then passes through a series of flash drums at varying pressures. Finally, depressurization will release the CO_2 from the solvent and the lean solvent is then recycled back to the absorber. The energy consumption for physical absorption is low as only the energy for pressurizing the solvent (light pumping) is required. The physical absorption is not economically competitive for low partial pressure of CO_2 because the capacity of physical solvents is strongly dependent on partial pressure (Kohl & Nielsen, 1997).

e) Chemical absorption

Chemical absorption process is based on a contact between the gas to be treated (feed gas) and an aqueous solution containing one of the above solvents. Acid gas in the feed gas is a weak acid which reacts with the alkanolamine or alkaline salt to give bisulfide (with H_2S) and bicarbonate (CO_2). In the chemical absorption, the CO_2 is absorbed and chemically react with the solvent. The chemical absorption takes place in a fractional column which is equipped with trays or packing. The gas enters the column at the bottom tray. The aqueous solution enters the column at the top tray. There is a heat of reaction between the solvent and the acid gas during the absorption, which is exothermic. The

treated gas water content will be higher than the feed gas water content since the treated gas exits the unit at a higher temperature than the feed gas. Chemical absorption processes are applicable for removing dilute concentration of CO_2 at low partial pressure. However, the challenge of this technology for CO_2 capture from power plant is due to high energy demand for solvent regeneration and solvent degradation. The solvent such as amine solution, aqueous ammonia and carbonate removers CO_2 from the gas stream by means of chemical reactions in the absorption column. The ideal chemical solvent should have the following characteristics (Davidson, 2007):

- Lower energy/cost for solvent regeneration
- Higher absorption rate
- Higher reactivity for CO_2 capture
- Better stability, less degradation and lower corrosivity
- Lower solvent cost
- Lower environmental impact

2.3 Amine based absorption process

2.3.1 Process

As mention in section 2.2, there are techniques available to remove CO_2 from gases mixture. Chemical absorption technology, amine based absorption is most effective for CO_2 removal from flue gas (Chakrawarti & Hunek et al., 2001). The reaction between CO_2 and amines will enhance the driving force for the separation even at low partial pressure of CO_2. The cost of this technology is most cost-effective by gaining high purity (<99%) CO_2 vapor from flue gases in a single step.

Figure 2-1 shows a simplified process flow diagram for chemical solvent-based acid gas treating. Cooled synthesis gas enters the bottom of an absorber where it contacts an amine solution. The treated gas exits at the top of absorber. Lean solution enters the top of the absorber and counter-currently contacts the synthesis gas using trays or packing, absorbing acid gas contaminants as it passes down the column. Warm rich solution leaves the bottom of the absorber and is routed to a regenerator. Steam stripping is used to remove acid gas from the solution. The hot lean solution is then cooled prior to returning to the absorber. A lean/rich cross exchanger is used to reduce the sensible heat load on the regenerator reboiler (Echt, 1997).

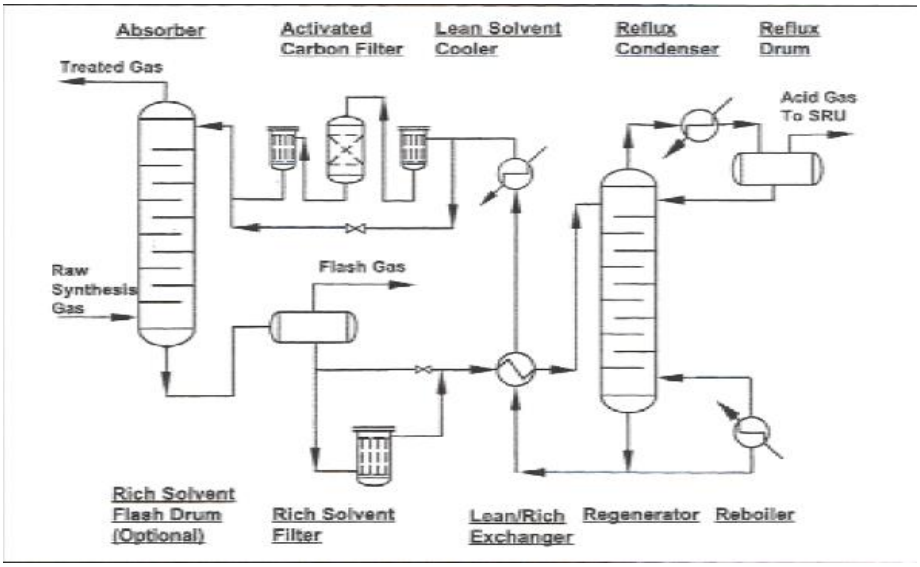

Figure 2-1: Process flow diagram of amine absorption process (Echt, 1997)

2.3.2 Categorization of Alkanolamines

According to Farmahini (2010), alkanolamines are a group of ammonia derivatives consisting at least one hydroxyl group and one amine group. Based on the number of substituents on the nitrogen atom, there are different subcategories for the amine group. Considering this general definition, it is normal to distinguish between the following classes of alkanolamines:

1. Primary alkanolamines: In this group of alkanolamines, nitrogen atom carries one substituent group (ethanol group) and two hydrogen atoms which are directly bonded to the nitrogen. MEA (monoethanolamine) is an example for this subcategory.

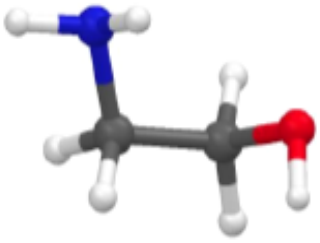

Figure 2-2: Molecular structure of monoethanolamine, C_2H_7NO

2. Secondary alkanolamines: In this subcategory, nitrogen atom is bonded to two ethanol group and one hydrogen atom. The best example is DEA (diethanolamine).

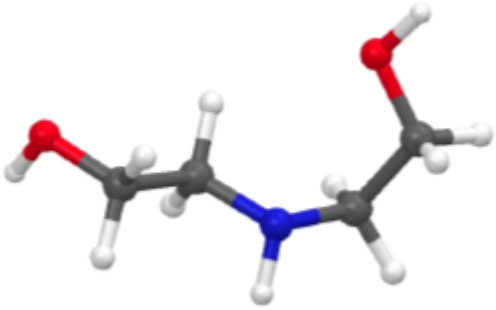

Figure 2-3: Molecular structure of diethanolamine, $C_4H_{11}NO_2$

3. Tertiary alkanolamines: The nitrogen atom of this alkanolamine is not bonded to any hydrogen atom but bonded to the alkyl or alkanol groups. MDEA (methyldiethanolamine) is an example for this subcategory.

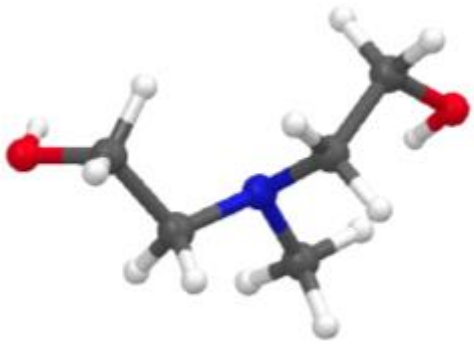

Figure 2-4: Molecular structure of methyldiethanolamine, $CH_3N(C_2H_4OH)_2$

In this simulation study, the alkanolamine used is methyldiethanolamine (MDEA). MDEA is an alkyl alkanolamine with colorless to yellow liquid tertiary amine compound. It is made up of 5 carbon atoms, 2 oxygen atoms, 13 hydrogen atoms and 1 nitrogen atoms. 2 ethanol molecules and 1 methane molecule are bonded to the nitrogen atom. It has an ammonia-like odor. It can undergo the typical reaction of amines and alcohols to form quaternary amine salts, soaps, and esters since it combines both characteristics. MDEA is considered slightly toxic MDEA is always used as an intermediate in the synthesis of numerous products such as coatings, polishes, textile lubricants, detergents, pesticides, personal products and pharmaceuticals (Dow, 2014).

In absorption process, the alkanolamines and their aqueous solutions will absorb carbon dioxide at lower temperatures and release the acid gases at higher temperatures.

This forms the basis for processes which separate carbon dioxide from gas streams. Normally, MDEA is used in tail gas treating for the removal of carbon dioxide. These units will, in most cases, permit 60 to 80% of the carbon dioxide to remain in the treated gas stream. MDEA is also used in natural gas plants for the bulk removal of carbon dioxide while producing a gas stream containing 0.25 grains hydrogen sulfide/100 scf. Bulk carbon dioxide removal can be realized with methyldiethanolamine when the CO_2:H_2S ratio ranges from 100 to 1,000 (Laffans Petrochemical, 2007).

2.3.3 Reaction between Amines and CO_2

Amine based absorption process technology is used to capture CO_2 in a large scale with amines as the solvent. There are three main type of amines can be used in absorption process. The three main types are primary amines (MEA), secondary amines (DEA) and tertiary amines (MDEA) (Nathalic et al., 2012).

The reaction between primary and secondary amines with CO_2 will form carbamate ion. Where else tertiary amines will form bicarbamate when react with CO_2. The reactions during the absorption process can be expressed as the equations below (Donaldson & Nguyen, 1980):

Primary or Secondary amines,

$$2R_1R_2NH + CO_2 \leftrightarrow R_1R_2NH^+ + R_1R_2NCOO^- \ (carbamate) \qquad \text{Equation 2-1}$$

Tertiary amines,

$$R_1R_2NH + H_2O + CO_2 \leftrightarrow R_1R_2NH^+ + HCO_3^- \ (bicarbamate) \qquad \text{Equation 2-2}$$

Interest of using MDEA which is a tertiary amine increased significantly in the last decade. The main advantages of MDEA instead of more traditionally used primary and secondary amines are its relatively high capacity, a low vapor pressure and small enthalpy of reaction with acid gases. Since the CO_2 reaction rate with MDEA is slow, the addition of small amounts of fast reacting amines is necessary to apply this process in flue gas treatment (Kierzkowska-Pawlak & Chacuk, 2010).

2.4 Molecular dynamic simulations

Molecular dynamics (MD) simulation is routinely used as a tool to investigate structure, dynamics and thermodynamics of materials and biological systems. It can be classified as a computer experiment which can provide average prediction results for a new theory or process (Frenkel et al., 2002). This computational technique originally started as the need to incorporate physical theory (electron and nuclei) to explain the details in chemistry (Berendsen et al., 1987). As Schlecht (1998) said in the preface of his book; ―Computer-aided molecular modelling doesn't exist for its own sake, but to contribute to scientific endeavour, and enable the scientist to work smarter. Therefore the computer simulation is a new emerging tool where the scientist has to consider due to its ability to produce molecular level information for scientists.

Molecular dynamic simulation is a numerical method of statistical molecular mechanics which has been developed to integrate Newton's second law by B.J Alder and T.E Wainwright in the 1950s. This integration simulates the dynamic environment of molecules by calculating each particle position and force acting on it during simulation. The law is expressed by Equation 2-3.

$$f_i = m_i a_i = m_i \frac{d^2 r_i}{dt^2} \qquad \text{Equation 2-3}$$

The mass of the particle represents m_i, a_i is acceleration and f_i is the force acting on the particle which can also be calculated using the Equation 2-4 where the $V(r_i)$ is the potential energy with respect to the position of the particle.

$$f_i = \nabla_i V(r_i) \qquad \text{Equation 2-4}$$

Simulation integrates the Newton equation of motion for each atom in the system with the structural constraints and molecular interactions such as intermolecular and intramolecular interaction (Allen & Tildesley, 1987). The intermolecular interaction is one of the forces incorporated which plays a significant role towards the system as well as process. Forces data will then be used to solve the velocity of atoms.

MD simulation will generate the trajectory in phase space which can be used to calculate macroscopic properties, structural properties and transport properties (Berendsen et al., 1987). Examples of macroscopic properties of the system are kinetic and potential energy, density, and pressure. While the structural property such as radial

distribution function can be used to describe the intermolecular interaction in the system. This interaction will then affect transport properties such as the diffusion coefficient. Nevertheless there are some limitations which are accuracy of the force field, simulation time and size of the system in the molecular dynamics simulation technique to produce acceptable results (Berendsen et al., 1987).

Simulation time that is too short may not be enough for the system to equilibrate and produce reliable results. A large system may require expensive calculation with adverse boundary effects and a system that is too small may not represent the real process with insufficient statistical accuracy (Berendsen et al., 1987). Therefore these factors should be taken into account before the simulation process begins.

2.4.1 Molecular Dynamic Time Integration Algorithm

A number of time integration algorithms have been developed to integrate the equation of motion. The time integration algorithm is a numerical method which is the engine of the MD program and it is based on the finite difference methods (Gunaratne, 2006). The time integration algorithm iterates the equations for *t* time and at a later time (t + Êt) and then produced a trajectory of the time evolution. There are a few common time integration algorithms such as the Verlet, Velocity Verlet and Leap-Frog algorithm.

The velocity of the Verlet algorithm solves the Verlet algorithm deficiency to calculate the velocity explicitly (Jang, 2007) which may affect the simulation with constant pressure. The velocity of Verlet requires a modest operation mode and storage, and allow the usage of a relatively long time steps duration as the position (*r),* velocities (*v*) and acceleration (*a*) are calculated at the same time with high precision (Rai, 2012) using Equation 2-5, 2-6 and 2-7. This factor has attracted most MD simulation software developers to use this algorithm beside its capability to conserve the energy with numerically stable and time reversible properties.

$$a(t+\delta t) = \frac{f(t+\delta t)}{m} \qquad \text{Equation 2-5}$$

$$r(t+\delta t) = r(t) + v(t)\delta t + \frac{1}{2}a(t)\delta t^2 \qquad \text{Equation 2-6}$$

$$v(t+\delta t) = v(t) + \frac{1}{2}[a(t) + a(r+\delta t)]\delta t \qquad \text{Equation 2-7}$$

There are some criteria for a good algorithm to integrate Newton's equations of motion:

1. Speed is not important since most of the time is spent on calculating non-bonded interactions and forces rather than integrating the equations of motion. For Verlet algorithm, it is fast but relatively unimportant for calculations.
2. Accuracy for large time steps is important because the longer the time step, the fewer evaluations of the energies and forces are needed. Verlet algorithm is not very accurate for long time steps since it requires only short time steps (Δt= 1fs) for simulations.
3. Energy conservation is an important criterion where one has to distinguish between short-time and long-time energy conservation. In general, one comes to the cost of the other. For Verlet algorithm, the short-term energy conservation is fair and, more important, it exhibits little long-term energy drift.
4. Newton's equations of motion are time reversible, and so should be the integration algorithms. Non-reversible algorithms will have serious long-term energy drift problems. For Verlet algorithm, time reversible is related to its little long-term energy drift.

There are several algorithms that are equivalent to the Verlet scheme. Leap Frog algorithm evaluates the velocities at half-integer time steps and uses the velocities to compute the new positions (Hinchliffe, 2008).

$$v\left(t-\frac{\Delta t}{2}\right)=\frac{r(t)-r(t-\Delta t)}{\Delta t} \qquad \text{Equation 2-8}$$

Here $v(t+\frac{\Delta t}{2})$ can be approximated via a Taylor series expansion so that $r(t+\Delta t)$ follows:

$$v\left(t+\frac{\Delta t}{2}\right)=v\left(t-\frac{\Delta t}{2}\right)+\Delta t\frac{f(t)}{m} \qquad \text{Equation 2-9}$$

$$r(t+\Delta t)=r(t)+\Delta t v(t+\frac{\Delta t}{2}) \qquad \text{Equation 2-10}$$

The Leap Frog algorithm give rise to the same trajectories as the Verlet algorithm since it is derived from the latter. Since the velocities and positions are not defined at the same time, the kinetic and potential energy are also not defined at the same time since we cannot directly compute the total energy in the Leap Frog scheme.

Velocity Verlet algorithm is similar to the Leap Frog algorithm but the velocity and position are calculated at the same time:

$$r(t+\Delta t) = r(t) + \Delta t v(t+\Delta t) + \frac{f(t)}{2m}\Delta t^2 \qquad \text{Equation 2-11}$$

$$v(t+\Delta\, t/2) = v(t) + \frac{f(t)}{2m}\Delta t \qquad \text{Equation 2-12}$$

$$v(t+\Delta\, t/2) = v(t+\Delta t) - \frac{f(t+\Delta t)}{2m}\Delta t \qquad \text{Equation 2-13}$$

$$v(t+\Delta t) = v(t) + \frac{f(t+\Delta t)+f(t)}{2m}\Delta t \qquad \text{Equation 2-14}$$

The new velocities can only be computed once $r(t+\Delta t)$, thus the forces $f(t+\Delta t)$ have been computed. It can be shown that the Velocity Verlet algorithm is equivalent to the basic Verlet algorithm.

For most MD applications, Verlet-like algorithms are perfectly adequate. Higher-order algorithms (i.e, algorithms that employ information about higher-order derivatives of the particles coordinates) allow to use longer time steps without loss of short-term accuracy. However, higher-order algorithms require more storage and the calculation of the computation of higher-order terms may be time intensive too. Moreover, higher-order algorithms are not time reversible, for example the so-called predictor-corrector algorithms, which are the most popular class of higher-order algorithms used in MD simulations.

2.4.2 Periodic boundary condition (PBC)

The MD simulation normally runs in a confined and finite system or boundary system. There are few types of boundary condition which can be implemented in the MD simulation such as vacuum boundary condition and periodic boundary condition. The vacuum boundary condition is the simplest choice that simulates the system at zero pressure as gas phase. In the simulations, it is not suitable for molecules with distorted shape (Gunsteren et al., 2001). Periodic boundary condition is the most popular choice of boundary conditions. These boundary conditions are used to simulate processes in a small part of a large system as shown in Figure 2-5.

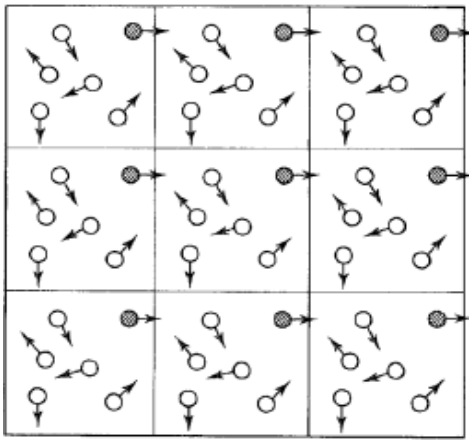

Figure 2-5: 2-D periodic boundary condition (Leach, 1996)

All atoms in the computational cell are replicated throughout the space to form an infinite lattice. If atoms in the computational cell have positions r_i, then the periodic boundary condition also produces mirror images of the atoms at positions defined as

$$\overrightarrow{r_{image}} = \vec{r_i} + l\vec{a} + m\vec{b} + n\vec{c} \qquad \text{Equation 2-15}$$

where *a*, *b*, *c* are vectors that correspond to the edges of the box, *l*, *m*, *n* are any integers from -∞ to +∞. Each particle in the computational cell is interacting not only with other particles in the computational box, but also with their images in the adjacent boxes.

Applying periodic boundary condition in MD simulation is useful because the bulk environment can be simulated by means of only limited number of molecules. In such a case, if for instance one molecule leaves the simulation box the same molecule emerges from opposite side of the box.

It is also important to decide about the box size in the simulation. In principle, size of the simulation box should be appropriately chosen so that the box can contain dimensions of the fluctuations or interactions which are supposed to be observed during the simulation (Leach, 1996). Most simulations are done with cubic computational cells, but other shapes, such as truncated octahedral or rhombic dodecahedral cells, are possible as shown in Figure 2-6. Non-cubic shapes can be used to eliminate the influence of the cubic symmetry on a shape of a crystal nucleus in a liquid.

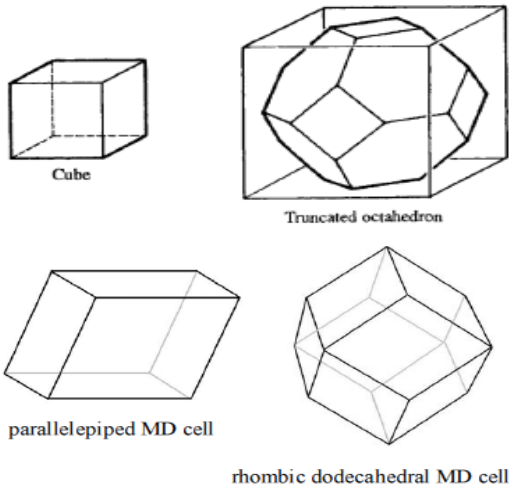

Figure 2-6: Different periodic cells in computer simulation

Limitations of the periodic boundary condition:

- The size of the computational cell should be larger than $2R_{cut}$, where R_{cut} is the cutoff distance of the interaction potential. In this case any atom *i* interacts with only image of any atom *j*. And it does not interact with its own image. This condition is called "minimum image criterion".
- The characteristic size of any structural feature in the system of interest or the characteristic length-scale of any important effect should be smaller than the size of the computational cell.

2.4.3 Force fields

Molecular dynamic simulation applies the molecular mechanics concept with forces as important elements. All the required potential energy functions are then incorporated into the force field concept and become the driving force of the simulation. Force field can be divided into three generations. The first generation of force fields is the generic force fields which has a wide coverage that provides reasonable prediction of molecule structures (Leach, 2001). The second generation force field is the force field that has been developed to improve the prediction quality rather than a wide application. The third generation force field produces high quality prediction and can also be applied to a wide range of disciplines including biochemistry and material science. This is because during the development of the third generation force field, the usage of quantum mechanical calculation or empirical method and fitted to experimental data were being employed. Hence, the force field selection is an important factor which can give

significant impact towards the simulation result. The force field for protein simulation for example may be not be suitable for inorganic simulation (Balbuena & Seminario, 1999).

The force field incorporates both intermolecular and intramolecular forces. In this study, the COMPASS (Condensed-phase optimized molecular potentials for atomistic simulation studies) force field was employed to simulate all the systems. This is because COMPASS is categorised as a third generation force field which is suitable in the simulation of organic molecules, inorganic gas molecules and common polymers. The simulation qualities can achieve up to nearly same as the industrial process. The COMPASS force field is a licenced force field which adds to the cross-coupling term for the prediction of vibration frequencies and structural variation (Schlecht, 1998). In addition, it also employed the LJ 9-6 (Equation 2-16) for E_{vdW} which is classified as softer in the repulsion region than LJ 12-6.

$$\Phi_{12}(r) = \varepsilon[2(\frac{r_m}{r})^9 - 3(\frac{r_m}{r})^6] \qquad \text{Equation 2-16}$$

where $\Phi_{12}(r)$ is the intermolecular pair potential between two particles or sites, ε is the depth of potential well, r_m is the distance at which the potential reaches its minimum and r is the distance between the particles.

2.4.4 Thermodynamic Ensemble

An ensemble is a collection of points in phase space where the points are distributed based on probability density (Allen & Tildesey, 1991) or it can be interpreted as a conceptual collection of identical systems with different microscopic states (atomic position, momenta) but having identical thermodynamic states (T, P, N) (York, 2007). There are three types of ensembles normally being employed in MD simulation. The first type is NVE ensemble or microcanonical ensemble which fixed the number of particles (N), volume (V) and energy (E). The second type is the NPT or Isobaric-isothermal ensemble where the number of particles (N), pressure (P) and temperature (T) are fixed during the dynamic process through the usage of pressure and temperature controller. The third type is the canonical ensemble (NVT) which allows energy and pressure to be fluctuated (Allen & Tildesey, 1991) and is widely used in biological molecular simulations. Amongst these ensembles, NVE and NPT are the ensembles chosen to be applied in this study.

2.4.4.1 NVE

The equilibration phase is the phase when the system evolves from the starting configuration to the stable or equilibrium system with energy conservation. In this study, NVE is used during this stage as this ensemble did not permit external forces to the system which is suitable to generate the state points of the system. This equilibration stage will continue until the values of set monitored properties such as energy become stable, even though there is a probability of energy drift during the ensemble generated (Rai, 2012).

2.4.4.2 NPT

The NPT is chosen for this study as it imitates the experimental condition such as the requirement to have the correct pressure and temperature in the simulation (York, 2007). It is also suitable for large systems. In addition, the simulation under NPT is able to measure the equation of state for the system even if the virial expression for the pressure cannot be evaluated (Frenkel & Smith, 1996). The NPT ensemble has been used by Gunther et al. (2005) to collect the data of predicting the extractability of hydrophilic solutes by modified carbon dioxide extraction technique.

2.4.5 Analysis Parameter

There are basically two types of the properties which are the structural properties and the dynamic properties that can be determined by the MD simulation. The structural properties are the object of the system which are not time dependent properties such as the radial distribution function (rdf). The dynamic properties of the system are the fluctuation and time dependent properties. It can only calculate through time specified trajectory data such as mean square displacement (msd). However, only radial distribution function (rdf) is focused in this simulation study as it can be used to visualize the molecular interaction (Adam et al., 2013).

2.4.5.1 Radial distribution function

Radial distribution functions (RDF) play an important role in the theory of simple fluids considering many thermodynamic properties in addition to the structure of the system can be identified from them (Leach 1996; Field 2007).

The radial distribution function (rdf) is a structural property to measure the probability of finding the neighbouring molecules at a particular distance r from the reference molecule (Anslyn & Dougherty, 2006). The rdf becomes the subject of interest

due to its ability to be expressed in thermodynamic function such as in the internal energy E which is the sum of kinetic and potential energy, U (Equation 2-17) (Hill, 1960).

$$E = \frac{3}{2}NkT + U \qquad \text{Equation 2-17}$$

where *E* is the internal energy, *N* is the number of particles, *k* is the Boltzmann constant, *T* is the temperature and *U* is the potential energy. By integrating the rdf function, the potential energy, *U* will be formed and the equation can be written as Equation 2-18.

$$\frac{E}{NkT} = \frac{3}{2} + \frac{\rho}{2kT} \times \int_0^\infty u(r)g(r,\rho,T)4\pi r^2 dr \qquad \text{Equation 2-18}$$

where *E* is the internal energy, *N* is the number of particles, *k* is the Boltzmann constant, *T* is the temperature, ρ is the density and *r* is the distance between the molecules.

There are RDFs in different levels such as the triple radial distribution functions or pair radial distribution functions. However, mostly RDF aims the latter. Pair radial distribution functions can be defined as a useful tool which measures "the probability of finding a particle as a function of distance from a typical particle relative to that expected from a completely uniform distribution, i.e. an ideal gas with density N/V (Jensen, 2006). Equation 2-19 demonstrates the above mentioned definition mathematically.

$$g(r,\delta r) = \frac{V}{N^2} \times \frac{<N(r,\delta r)>_M}{4\pi r^2 \delta r} \qquad \text{Equation 2-19}$$

where $g(r,\delta r)$ is dimensionless pair distribution function, $N(r,\delta r)$ is the number of particles in spherical shell, subscript *M* signifies the average (mean) value, *V* is volume of the system , *N* is number of particles in the system and $4\pi r^2 \delta r$ is volume of the spherical shell with thickness δr.

The rdf is important for three main reasons. Firstly, it is useful for pairwise additive potentials, knowledge of the rdf is sufficient information to calculate thermodynamic properties, particularly the energy and pressure. Secondly, the rdf is very well developed integral equation theories that permit estimation of the rdf for a given molecular model. Last but not least, the rdf can be measured experimentally, using neutron-scattering techniques. **Figure 2-7** shows the schematic explanation of g(r) of a monoatomic fluid. The atom at the origin is highlighted by a black sphere. The dashed

regions between the concentric circles indicate which atoms contribute to the first and second coordination number of shells respectively (Adam et al., 2013).

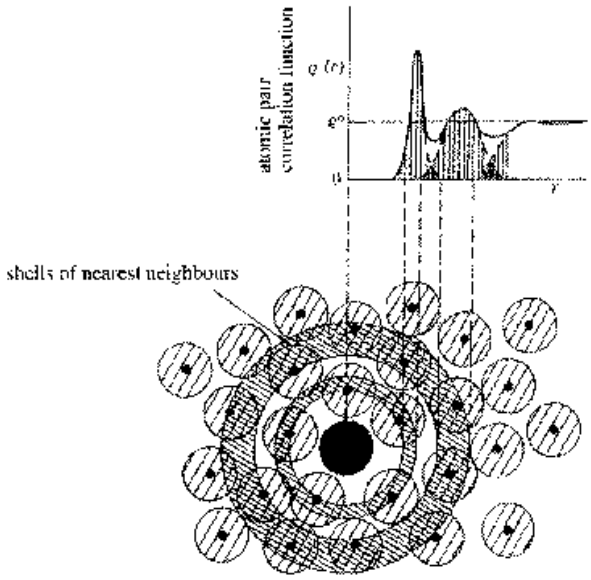

Figure 2-7: Schematic explanation of g(r) of a monoatomic fluid

The g(r) pattern basically depends on the phase of the system. The ideal gas will approach g(r) = 1. These patterns can be seen in Figure 2-8. Figure 2-8 (a) represents the g(r) in gas, (b) in liquid and (c) in solid phase.

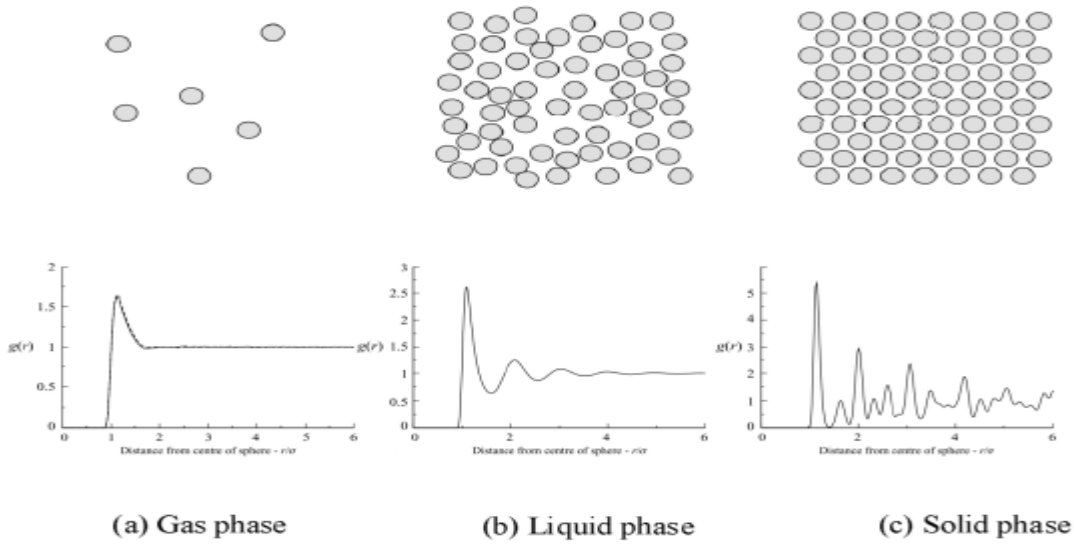

Figure 2-8: The atomic configuration and rdf pattern for (a) gas, (b) liquid and (c) solid phase (Barret & Hansen, 2003)

From Figure 2-8, the rdf pattern for solid phase fluctuates more frequently as compared to liquid and gas phase. According to kinetic molecular theory of matter, the atoms of solid phase are arranged accordingly so they will vibrate constantly. Vibration between the atoms will cause repulsive force against each other. Therefore, many fluctuations occur as shown in Figure 2-8 (c). Since liquid atoms are just arranged closely to each other and gas atoms are far apart from each other, so their rdf patterns are quite stable as compared to solid phase.

2.4.1.1 Molecular diffusion

Molecular diffusion can be describe as the spread of molecules through random motion. For a molecule M in an environment where viscous force dominates, its diffusion behaviour can be described by the diffusion equation as below.

$$\frac{\delta}{\delta t}c(r,t) = D\nabla^2 c(r,t) \qquad \text{Equation 2-20}$$

where $c(r,t)$ is a function that describes the distribution of probability of finding M in the small distance of the point *r* at time *t*. *D* is the diffusion coefficient and *c* is the concentration (Junmei Wang, 2012).

Molecular diffusion always related with the mean square displacement. Mean square displacement (MSD) of atoms in a simulation can be easily computed by its definition

$$MSD = \langle |r(t) - r(0)|^2 \rangle \qquad \text{Equation 2-21}$$

where $\langle |r(t) - r(0)|^2 \rangle$ are the average distance over all the atoms. Meanwhile MSD consist the information on the atomic diffusivity. If the environment is in liquid state, MSD grows linearly with time. So, it becomes useful to characterize the environment system behaviour in term of slope, which is the diffusion coefficient *D*:

$$D = \lim_{t \to \infty} \left(\frac{1}{6} (\langle |r(t) - r(0)|^2 \rangle) \right) \qquad \text{Equation 2-22}$$

the 6 indicate the six possible direction of diffusion for atoms when in consideration of three dimensional system. It must be change to 4 if the system is two dimensional (Furio, 1997). Rearrangement of the equation is then expressed as the equation below:

$$\langle r^2 \rangle = \lim_{t \to \infty} (6Dt)$$ Equation 2-23

The diffusion coefficient D can be obtained from a plot of the MSD versus time as shown in Figure 2-9. The gradient of the line will be the value of $\langle |r(t) - r(0)|^2 \rangle$.Hence, the value of coefficient diffusion, D of a molecule will be the gradient of the graph divided by 6 (Stefan, 2001).

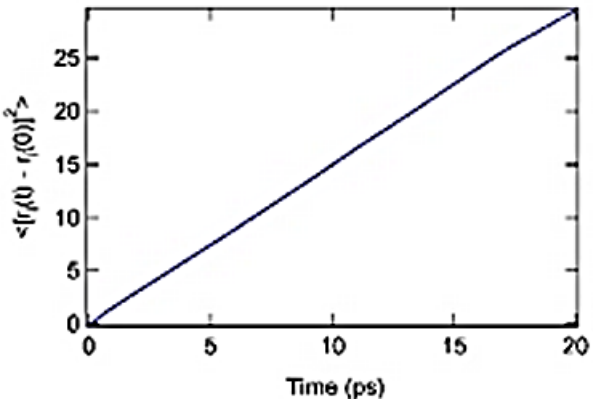

Figure 2-9: Graph of MSD versus time

2.5 Molecular Mechanics (MM)

Molecular mechanics was developed to describe molecules in terms of "bonded atoms", which have been distorted from some idealized geometry due to non-bonded van der Waals and Coulombic interactions (U. Burket & N.L. Allinger, 1982; A.K. Rappe & C.J. Casewit, 1997). The success of molecular mechanics models depends on a high degree of transferability of geometrical parameters from one molecule to another, as well as predictable dependence of the parameters on atomic hybridization. It is categorized under statistical mechanics model which consider the valence and bonding concept and ignores the electron effect which is central to the quantum mechanics approach. In this concept, the molecule is being considered as a system of rigid balls that are connected via springs. In this approach, molecular geometry will be affected by the non-bonded interactions (Hehre, 2003), rather than the bonded or intramolecular interactions. This ideal geometry of the molecules has its suitable steric energy or the energy due to the geometry of molecule (Shattuck, 2008) or is can be calculated from Equation 2-24. Steric energy is the energy of the molecules which the inherent form of energy between the real molecules and the relative forms (Hehre, 2003). This molecular mechanics "energy" of a molecule is described in terms of a sum of contributions arising from distortion from

"ideal" bond distances ("stretch contributions"), bond angles ("bend contributions") and torsion angles ("torsion contributions"), together with contributions due to "non-bonded" (van der Waals and Coulombic) interactions.

$$E_{steric\ energy} = E_{stretch} + E_{bend} + E_{stretch\text{-}bend} + E_{out\ of\ plane} + E_{torsion} + E_{van\ der\ waal} + E_{qoulumbic}$$

Equation 2-24

The steric energy of the molecule is contributed from two main interactions which are intramolecular and intermolecular. The first 5 energy terms in the Equation 2-24 are under intermolecular interaction or the bonded energy terms while the rest of last 2 terms in the Equation 2-24 are the intramolecular interaction energy terms.

Molecular mechanics is the core concept employed during the establishment of the potential function or the force field (Machida, 1999). The force field is the main operating parameter in molecular dynamics simulation. The different force fields may produce different simulation results. The force field has been discussed in previous section 2.4.3.

2.5.1 Molecular modelling

Molecular modelling concerns various techniques which are widely used in molecular design technology within chemical, pharmaceutical and agrochemical industries. Molecular modelling involves modelling of the various types of potential interactions by which behaviour of the molecules are explained. As mentioned earlier, in molecular mechanics (MM), classical definitions of potential energy are used. In this regard, two main types of molecular interactions are distinguished: intermolecular interactions which occur among the individual molecules and intra-molecular interactions that are contributions of atoms into the potential energy within each molecule.

2.5.1.1 Intramolecular interactions

When atoms join to form molecules, they are held together by chemical bonds. The type of bond and the strength of bond depend on the atoms that are involved. These bonds are called intramolecular forces because they are bonding forces inside the molecule. Intramolecular forces are defined as the force between the atoms of a molecule which holds them together (Zumdahl & Decoste, 2013). Therefore the intramolecular forces are stronger than the intermolecular forces which determine the stability of the

molecule. Covalent, ionic and metallic bonds are the types of chemical bonds that can exist between atoms inside a molecule. In this study, the bond between atoms inside the solute and solvent molecules involve the covalent bond type.

In an organic compound, the intramolecular or covalent bond forces will contribute to the bonded energy terms which can be divided into $E_{stretch}$ (bond term), E_{bend} (angle term), $E_{out\ of\ plane}$ (improper dihedral term) and $E_{torsion}$ (torsion term) (Shattuck, 2008). The bond term or E stretch is the energy required to stretch the bond from its equilibrium length. The angle term (E bend) is the energy required to bend the bond from its equilibrium angle. The E torsion (torsion term) is the energy needed to rotate the bond. The improper dihedral term or E out of plane is the energy required to deform a planar group of atom from its equilibrium angle. All of these energy terms is used by the bond in order to resist the changes and revert to their equilibrium position which is of paramount importance during parameterized force field.

2.5.1.2 Intermolecular interactions

Intermolecular interaction is the interaction between two molecules when approaching each other or non-bonded interaction. This interaction is those bonds that hold molecules together. This interaction normally defines the compound phase whether it is in solid or liquid phase (Zumdahl & Decoste, 2013; Ebbing & Gammon, 2009). There are few types of intermolecular forces such as dipole-dipole interaction, London dispersion and other interaction which will be discussed in subsequent subsections. The strength of the intermolecular forces is important because they affect surface tension and properties such as melting point and boiling point. The strength of the intermolecular forces increases as the size of the molecule increases. It also can affect the viscosity of the liquid (Ebbing & Gammon, 2009).

2.5.1.2.1 Electrostatic interactions and Ewald summation

Electrostatic interactions as the long range interactions are a group of non-bonded interactions which follow the Coulomb's law. Partial or formal charges (in the ionized molecules) of the atoms cause this type of interaction. Electrostatic interactions can be either attractive or repulsive, depending on the signs of the charges. Therefore mutual potential energy is defined by Equation 2-25.

$$U_{AB} = \frac{1}{4\pi\varepsilon_r\varepsilon_0} \times \frac{q_A q_B}{R_{AB}} \qquad \text{Equation 2-25}$$

where ε_0 is a vacuum permittivity and ε_r is a relative permittivity.

Since the interactions over very long distances within the periodic boundary condition are negligible, so calculation of the electrostatic interactions between all the atom pairs is not computationally favourable. *Cut-off* distances are proposed to be employed to reduce the computational requirement reasonably. However, truncation of the interactions beyond the cut-off distance does lead to some serious mathematical problems, such as discontinuity within the interaction profile. The *Ewald summation* method is utilized in order to diminish the computational effort as low as possible and to simultaneously keep the accuracy high enough. This method is able to calculate the electrostatic energy "exactly" (Jensen 2006) and to include "all the effects of long-range forces into a computer simulation" (Leach 1996).

Application of Equation 2-26 for all the atom pairs within the periodic boundary condition can be redefined as following (Leach 1996).

$$U_{el} = \frac{1}{2}\sum_{n=0}^{\infty}\sum_{i=1}^{N}\sum_{j=1}^{N}\frac{q_i q_j}{4\pi\varepsilon_0|r_{ij}+n|} \qquad \text{Equation 2-26}$$

A cluster of cubic cells has been assumed so that n is position of the box within the cubic lattice, *N* is the number of charges in each box and r_{ij} is the minimum distance between charge *i* and *j*. The prime on the first sum signifies interactions of i = j are excluded for n = 0 (Farmahini, 2010).

2.5.1.2.2 Short range interaction

Short range interactions are a variety of dipole-dipole, induced dipole and dispersion interactions in combination with the repulsive contribution. The first three contributions have attractive effect between the dipoles (permanent, induced or instantaneous). In addition, dispersion interaction is also known as London forces. London forces is a quantum mechanical phenomenon caused by instantaneous fluctuations of the electron distribution which contribute to the formation of temporary dipole moments. These dipole moments can induce some other dipoles among the electron distribution of the neighboring atom which contribute to the dispersion interactions.

Electron cloud overlap leads to strong short range repulsive forces since electron density and nuclear shielding are reduced. This in turn increases the coulombic repulsion between the positively charged nuclei (Jensen, 2006). This force partly prevents a crystal lattice from collapsing in on itself and falls off exponentially with respect to inter-atomic distances (Hinchliffe, 2008). However, there is also a quantum mechanical effect before the nuclear repulsion becomes significant because the electrons are forced to occupy a smaller portion of space. Since the electrons must maintain orthogonal orbitals, the energy states increase in energy. This is known as the orthogonalisation or Pauli repulsion. There is a contrasting longer range attractive inter-action at larger interatomic distances arising from the formation of instantaneous dipoles between adjacent electron clouds. This effect, known as the van der Waals interaction, is clearly also quantum mechanical in origin (Adam et al., 2013). A famous mathematical description which models the short-range interactions is Lennard-Jones (L-J) potential model explained by Equation 2-27.

$$\Phi_{ij}(r_{ij}) = \frac{A_{ij}}{r_{ij}^{12}} - \frac{B_{ij}}{r_{ij}^{6}} \qquad \text{Equation 2-27}$$

where A_{ij} and B_{ij} are the variable attractive and repulsive parameters respectively, is often used to model non-bonded interactions such as rare gas solids. Here, is the minimum potential energy or in other words the maximum attraction potential, known as potential well depth, while is the distance at zero potential and R is inter-atomic distance. The first term with the power of 12 represents the repulsive interaction which falls off dramatically as the distance increases. Repulsion interaction can be illustrated better by an exponential function but it has been simplified here by using the 12^{th} power of the inverse of distance. The second term in L-J potential expression represents the attraction interaction which falls off much slower than the repulsion one.

Considering the above mentioned behaviour of the L-J potential, at long distances they are totally negligible. Therefore, molecular simulators usually prefer to truncate them when interacting particles are very far from one another in order to save the computer time. However, as stressed earlier, this so called cut-off option can give rise to some serious mathematical problems based on the discontinuity issue. As such, some circumventing methods are essential. Through these methods, the molecular interactions can be explained in easier way (in graph form) as shown in Figure 2-10 and Figure 2-11.

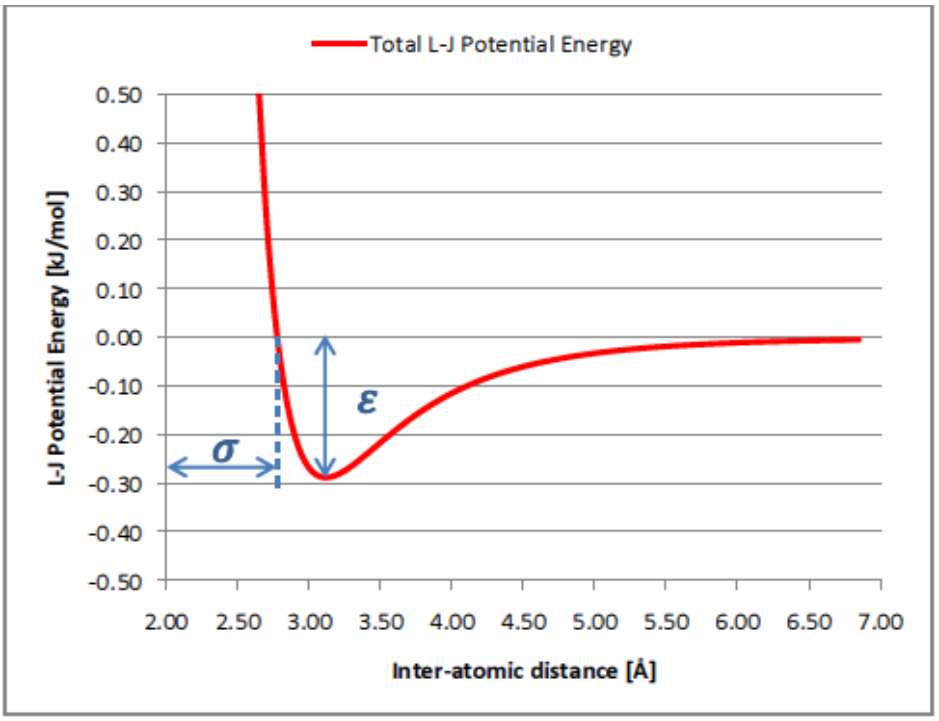

Figure 2-10: L-J power of 12-6 potential energy for Neon atom

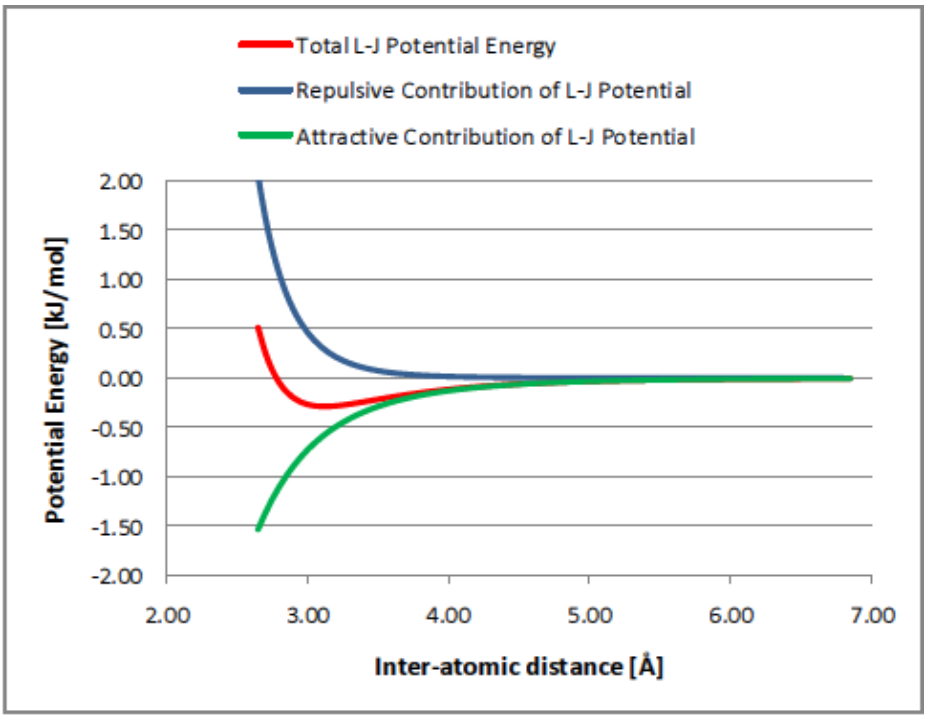

Figure 2-11: L-J power of 12-6 potential energy for Neon atom with its repulsive and attractive contributions

Besides that, there are other mathematical descriptions which model the respective interaction. For example, a Morse potential can be used to describe wider ranges of separation,

$$\Phi_{sr}(r_{ij}) = D_{ij}[1 - \exp(-\beta_{ij}\{r_{ij} - r_0\})]^2 \qquad \text{Equation 2-28}$$

where D_{ij} is the dissociation energy of the bond and β_{ij} is a variable parameter that can be determined from spectroscopic data. This type of model is particularly useful in chemical systems to model bonded covalent interactions and the O-H species.

If the r^{12} term in the Lennard-Jones potential is replaced by a more complex dual parameter exponential term the Buckingham potential form results,

$$\Phi_{sr}(r_{ij}) = A_{ij} \exp\left(\frac{-r_{ij}}{\rho_{ij}}\right) - \frac{C_{ij}}{r_{ij}^6} \qquad \text{Equation 2-29}$$

where A_{ij} and p_{ij} describe components of the repulsive interaction and C_{ij} describes the attractive interaction. A_{ij} and p_{ij} are thought to relate to the number of electrons and the electron density respectively, while C_{ij} is meant to represent the van der Waals interaction. In the case where ions have small polarisabilities the C-term is often omitted giving rise to a Born-Mayer potential model (Hafemeister & Zahrt, 2004). The Buckingham and Born-Mayer potentials have been used successfully in the excellent work of Grimes and co-workers to model a wide range of crystal structures and ionic species.

Finally it is worth mentioning the original simple short range potential for ionic systems (Born & Huang, 1954),

$$\Phi_{sr}(r_{ij}) = \frac{A_{ij}}{r_{ij}^n} \qquad \text{Equation 2-30}$$

where A_{ij} is a variable parameter and the optimum value of *n* was determined to be approximately 9.

The classification of the short range interaction used here is somewhat generalised since the van der Waals interaction will operate over several atomic distances. However, it is often convenient to think of it as a short range interaction since it reduces rapidly with r_{ij}. As such, the interaction is often considered zero beyond a sensible cut-off distance.

2.5.1.2.3 Dispersion forces

According to Israelachvili (2011), dispersion forces make up the most important contribution to the total van der Waals forces between atoms and molecules. Dispersion force act like the gravitational force between all atoms and molecules. They play a role in a host of important phenomena such as adhesion; surface tension; physical adsorption; wetting; the properties of gases, liquids, and thin films; the strengths of solids; the flocculation of particles in liquids; and the structures of condensed macromolecules such as proteins and polymers. Their main features may be summarized as follows:

1. They are long-range forces and, depending on the situation, can be effective from large distances (greater than 10 nm) down to interatomic spacing (about 0.2 nm).
2. These forces may be repulsive or attractive, and in general the dispersion force between two molecules or large particles does not follow a simple power law.
3. Dispersion forces not only bring molecules together but also tend to mutually align or orient them, though this orienting effect is usually weaker than with dipolar interactions.
4. Dispersion forces are not additive that is the force between two bodies is affected by the presence of other bodies nearby. This is called the non-additive of an interaction.

2.6 Quantum Mechanics (QM)

Quantum mechanics is a branch of physics which deals with physical phenomena at nanoscopic scales where the action is on the order of the Planck constant. It departs from classical mechanics primarily at the quantum realm of atomic and subatomic length scales. Quantum mechanics provides a mathematical description of much of the dual particle-like and wave-like behavior and interactions of energy and matter. Quantum mechanics provides a substantially useful framework for many features of the modern periodic table of elements including the behavior of atoms during chemical bonding and has played a significant role in the development of many modern technologies (Chester & Marvin, 1987). Hence, the state of a system is fully described by the wave function $\Psi(r_1, r_2, \dots, t)$ which contains information about all the properties of the system that is opened to experimental determination (Atkins & Friedman, 2005).

QM is the fifth and final postulate describing time dependent "dynamical evolution of the wave function". This is the called the Schrödinger equation represented by Equation 2-31 as a partial differential equation,

$$i\hbar\frac{\partial\Psi}{\partial t} = H\Psi \qquad \text{Equation 2-31}$$

where *H* is the Hamiltonian operator corresponding to the total energy of the system and is the reduced Planck's constant. This is equivalent to Equation 2-32 presenting the total kinetic and potential energies explicitly in Cartesian coordinate system.

$$i\hbar\frac{\partial\Psi}{\partial t} = -\frac{\hbar^2}{2m}\nabla^2\Psi + V(x,y,z)\Psi \qquad \text{Equation 2-32}$$

Exact solution of the Schrödinger equation for large systems is impossible and for small systems even very complicated. Therefore, another basic concept named atomic orbitals (AO) is introduced. The atomic orbitals are "one-electron wave functions in atoms" labelled by letters s, p, d, f, (...) so that for instance an electron occupying a s-orbital is called s-electron. Similarly for other orbitals there are p-electrons in p-orbitals and so on (Atkins & Friedman, 2005).

If the exact information of wave function Ψ_{nlm_l} is known, the Schrödinger equation can be solved easily where n, l and m_l are called the quantum numbers. These quantum numbers are introduced as below.

n is the principle quantum number ranging from 1, 2, 3… specifying the number of electronic shells on the atomic structure. This number also decides about the energy of the shell according Equation 2-33 and controls range of the l quantum numbers from 0 to $n-1$.

$$E_n = -\left(\frac{Z^2\mu e^4}{32\pi^2\varepsilon_0^2\hbar^2}\right)\left(\frac{1}{n^2}\right) \qquad \text{Equation 2-33}$$

where Z is the atomic number, μ is reduced mass and is vacuum permittivity.

Each electronic shell is composed of n number of subshells which are the atomic orbitals with quantum number l. l is also defined as the orbital angular momentum quantum number giving the orbital angular momentum of the electron through Equation 2-34. Moreover, this quantum number controls the range of between – l and l.

$$Magnitude\ of\ the\ angular\ momentum = \{l(l+1)\}^{\frac{1}{2}}\hbar \qquad \text{Equation 2-34}$$

m_l is called magnetic quantum number, and is defined as component of the orbital angular momentum of an electron. This quantum number is represented by individual orbitals so that there are $2l + 1$ individual orbitals in each subshell (Atkins & Friedman, 2005).

2.6.1 Partial atomic charges

Partial atomic charges are used in molecular mechanics force fields to compute the electrostatic interaction energy using Coulomb's law. They are often used for a qualitative understanding of the structure and reactivity of molecules. Information such as atomic charge in a given species must be identified to predict the stability, solvation energetics of various molecules, course a particular reaction, and its interaction between molecules. It is very problematic to calculate the partial atomic charges within the molecules since positions of the electrons around the atoms are not fixed and other neighbouring atoms continuously affect the electrons especially when there is a solvent environment available. Therefore, a simple scheme called Mulliken population analysis (MPA) is introduced to partition the electronic distribution among the atoms based on the contribution of atomic orbitals (Mulliken, 1955). MPA is very dependent to the size of basis sets but it neglects the effect of electronegativity of various atoms since it assumes that the electrons are divided evenly along the bond length between different atoms (Cramer, 2004).

Application of a symmetric orthogonalization scheme named Löwdin population analysis (LPA) is proposed to avoid the deficiency of MPA on the non-orthogonality in regard with the atomic orbitals. LPA can be defined by Equation 2-35.

$$N_i = \sum_i S_{ii}^{\frac{1}{2}} P_{ii} S_{ii}^{\frac{1}{2}} \qquad \text{Equation 2-35}$$

where N_i is atomic population, P_{ii} is density matrix, S_{ii} is overlap matrix, and $S_{ii}^{\frac{1}{2}} P_{ii} S_{ii}^{\frac{1}{2}}$ is the Löwdin density matrix. Löwdin charges themselves are not stable with very large basis functions such as diffuse functions. To alleviate this problem Redistributed Löwdin population analysis (RLPA) has been proposed. This method modifies the part of the LPA

that comes from diffuse functions and therefore diminishes sensitivity of this method towards the diffuse functions (Thompson, 2002).

MPA and LPA scheme are categorized as class II charge models which molecular wave functions (MO) are partitioned into contributor atomic orbitals (AO). Class I charged model is developed only for neglect of diatomic differential overlap theory. Class III charge model stands for physical observables. This study will focus on class IV charge model which is the combination of class II and class III charge models to provide more accurate charge distribution.

3 METHODOLOGY

3.1 MD simulations methods

MD simulation is an essential technique to study a variety of molecular properties including molecular diffusion. Diffusion process not only can be studied in atomic details, but also under various thermodynamic conditions that is unreachable by experiments. This research specifically undertakes studies of CO_2 absorption in aqueous alkyl alkanolamine-based solvent which is methyldiethanolamine (MDEA) in molecular scale to provide more insight into the molecular interactions involved in the absorption process.

In order to replicate true behaviour of the system in actual life, speciation of the system needs to be determined accurately. Speciation of the solution will be specified accurate enough from literature review which can be used as initial composition of the system, i.e. CO_2, water and MDEA. Once speciation of the system is determined, modelling of the decided molecules/ species can be started using Molecular Dynamic (MD) technique of the specified molecules or species for the solution.

Molecular Dynamic (MD) simulation works by treating a microscopic replication of the macroscopic system as a manageable box of the molecules in order to predict the configurations and properties of the system in any time in future (Leach 1996). MD employs an initial configuration of the molecules as input, and then computes the molecular forces based on interaction parameters of a given force field. Subsequently, it determines velocities and positions of the molecules by integrating the Newton's law of motion. Data collected from any preceding step is used to calculate the new forces, velocities and positions for the ensuing configuration after a very small time interval. This procedure is followed by the same cycle to predict the configuration of the system at any time in future. This means that MD generates a *Trajectory* of the system with respect to time. Having this information, thermodynamic averages of the system can be calculated by applying statistical mechanics approach to resemble the thermodynamic properties of the macroscopic system of interest.

Procedure for modelling of the molecules involves three main steps. First of all interaction parameters have to be decided through a suitable force field, second optimization of the molecular geometry and at last calculation of partial charges.

Molecular dynamics (MD) simulation approach was chosen to investigate the molecular distribution of the system inside the absorption solution (Hinchliffe, 2000).

In order to perform the MD simulation in current study, the simulation box will be divided into two different parts. For the first part, it will be occupied by liquid phase (including the aqueous amine solution) and the second part will contain the gases components (CO_2). Both of the parts will be brought into contact with one another within a gas-liquid interface, so that the absorption process could take place across this interfacial surface (Belonoshko, 1998).

MD simulation will be performed in thermodynamic conditions of the systems which will be set to be closed to the one in absorption unit to be able to replicate the real absorption characteristics. The thermodynamic conditions can be under NVE (constant number of moles, volume and energy), NPT (constant number of moles, pressures and temperature) and NVT (constant number of moles, volume and temperature) assemble up to 5 ns. The movement of each molecule will be integrated according to the second Newton's Law to achieve the equilibrium (Keffer & Baig et al., 2005)

The effect of molecular structure i.e. steric hindrance and functional group on solvent properties such as basicity will be investigated. The simulation results will be interpreted in terms of radical distribution function, diffusion coefficient and simulation validation. The following Figure 3-1 shows the process flow in simulating the model at molecular level.

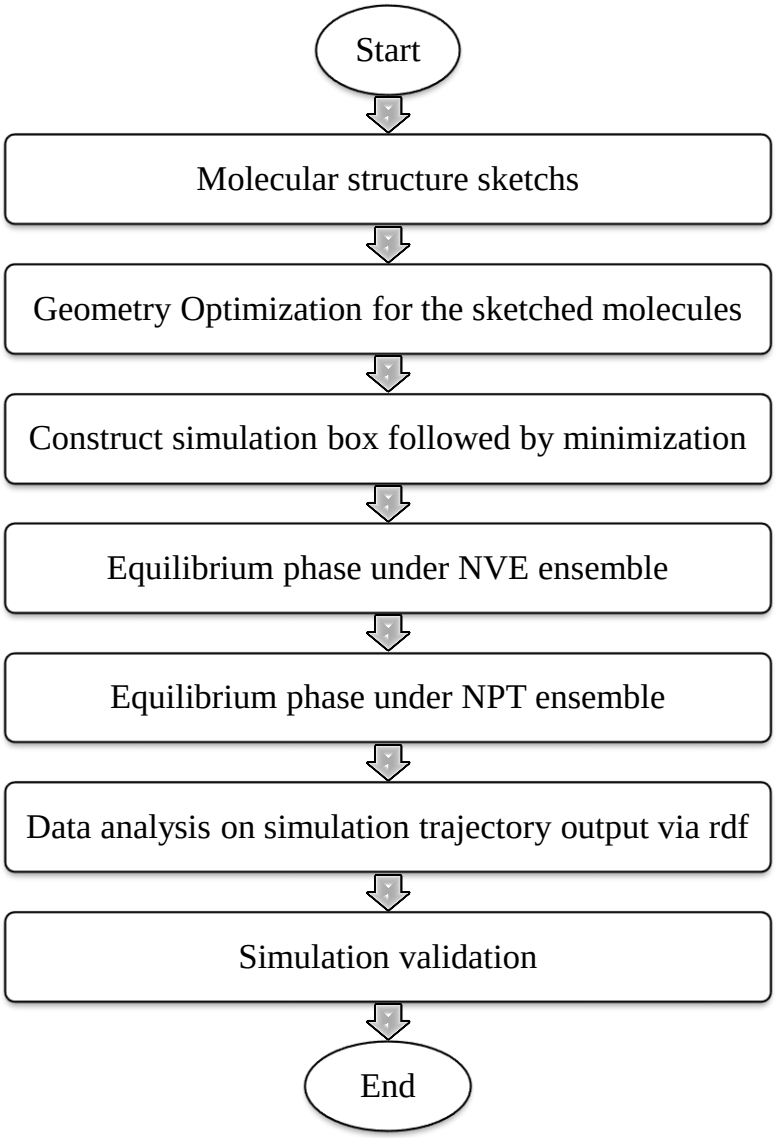

Figure 3-1: Summarization of MD simulation procedure

3.2 Software

In this MD simulation, the Material Studio software package 6.1 has been used to simulate the molecules (MDEA, H_2O and CO_2). It is a very useful tool to comprehend and reveal the molecular interaction between molecules during the absorption process. The acid gas used in study is carbon dioxide and the solvent is methyldiethanolamine (MDEA). By applying Newton's second law, the dynamic aspect of the system will be simulated and the coordinate system will be used to calculate radial distribution function (rdf) (Anslyn & Dougherty, 2006), and diffusion coefficient. This will be used to shows how strong the molecule interaction and even which atoms of the molecules attracted the most between the solvent and acid gas (Matteoli et al., 1995).

4 RESULTS AND DISCUSSIONS

4.1 Radial Distribution Function (RDF) analysis

4.1.1 Primary system

Three stages of simulation are established to study the intermolecular interaction of MDEA absorption for CO_2 capture. The first stage name primary system involved a single molecule. Molecular dynamic simulation for a single component is conducted at temperature 45°C. Figure 4-1 shows the atomic structure of carbon dioxide where the C3 indicates the carbon atom, while O1 and O2 indicate the first oxygen atom and the second oxygen atom respectively.

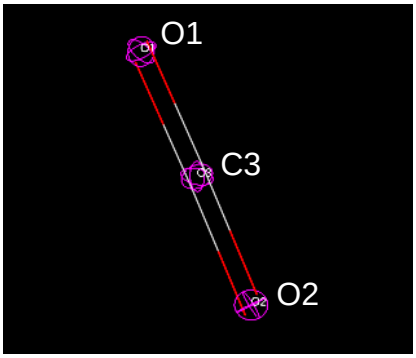

Figure 4-1: Atomic structure of carbon dioxide

4.1.1.1 Carbon dioxide and water

From Figure 4-2, g(r) is the radius of gyration (root mean square distance of the objects' parts from its centre of gravity) and r(Å) is the forces between molecules or atoms. As shown in Figure 4-2, at a very small distance, r, the function g(r) is essentially zero since the atoms cannot strongly overlap their electronic shells. The peak repulsive between the carbon atom (C3) and second oxygen atom (O1) as shown in Figure 4-2 (see red line) occurred at 4.75 Å. Therefore, the strongest interaction with the closest neighbouring molecule occurs between the carbon atom (C3) and oxygen atom (O2).

The trend line for the RDF plot shows some fluctuations closed to g(r) = 1 for the distance greater than 10Å. As the distance between the molecules is increased, the interaction between the molecules will become weaker since the RDF plot shows a low oscillation of g(r).

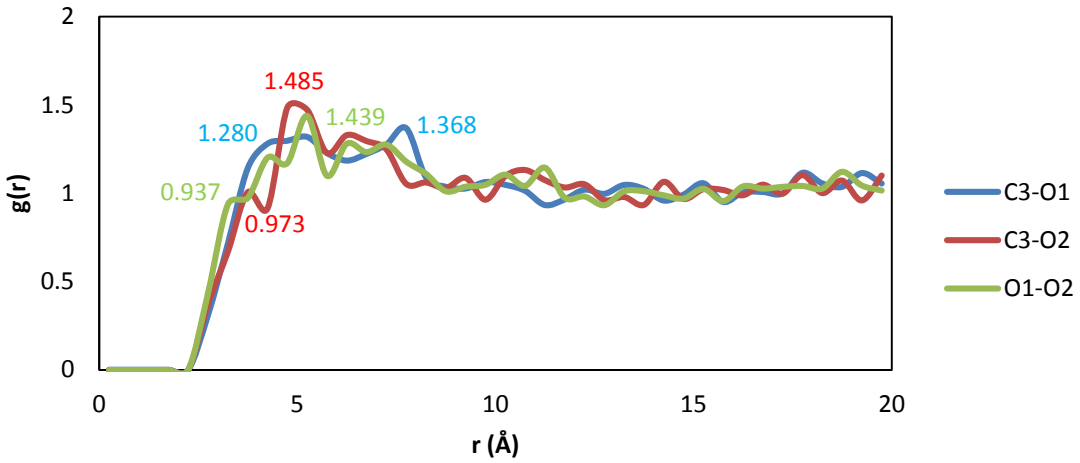

Figure 4-2: Molecule interaction in pure CO_2 molecules at 45℃

Figure 4-2 shows that the intermolecular interaction of C3CO2-O1CO2 has reached the first peak at 4.25Å but the highest peak is at 7.75Å (see blue line). This means that this is the highest potential distance, r for the molecules to interact with each other. At long distance, the trend line of interaction would reach g(r) ≈1 which indicates there is no long range order and the intermolecular interactions are almost negligible with any atoms. The same theory is applied to the other atom interactions. Table 4-1 shows the data of function g(r) peak of different atoms' interaction.

Table 4-1: Data of function g(r) peak for different atoms' interaction of pure CO_2 at 45 ℃

Type of interactions	First peak	Highest peak
C3—O1	1.280	1.368
C3—O2	0.973	1.485
O1—O2	0.937	1.439

From Figure 4-3, the intermolecular interaction of CO_2 at 40°C has less fluctuation compared to 45°C. From Table 4-1 and Table 4-4-2, the first potential interaction of CO_2 at 40°C is always higher than the first potential interaction of CO_2 at 45°C. As from the C3—O1 interactions, CO_2 at 40°C has 1.4963 to have potential interactions between two atoms as compared to CO_2 at 45°C which has only 1.280 to have potential interactions between two atoms.

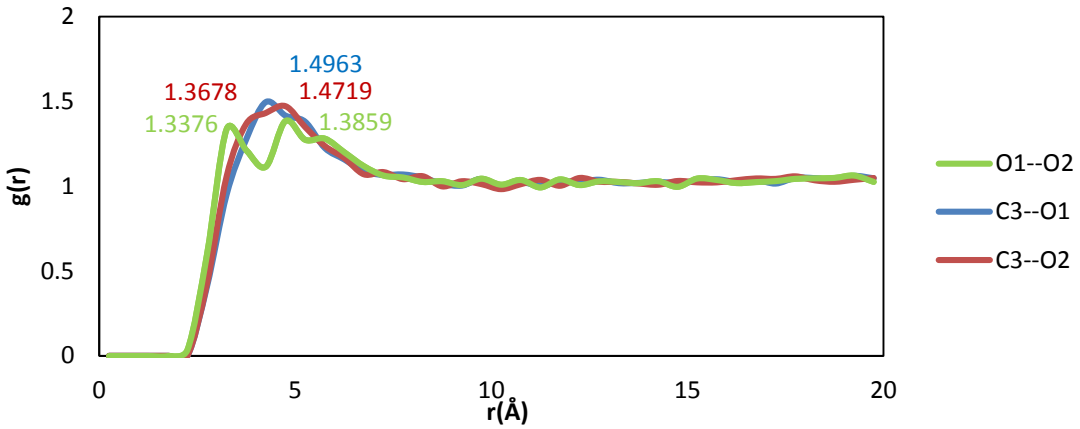

Figure 4-3: Molecule interaction in pure CO_2 molecules at 40°C

Table 4-4-2: Data of function g(r) peak for different atoms' interactions of pure CO_2 at 45 ℃

Type of interactions	First peak	Highest peak
C3—O1	1.4963	1.4963
C3—O2	1.3678	1.4719
O1—O2	1.3376	1.3859

When the temperature increases, the kinetic energy of the molecules will increase too. Collision between the molecules will occur more frequently and cause higher repulsive force. Higher repulsive force will cause the distance between two molecules to be bigger. So, carbon dioxide at 40°C always has a higher g(r) value than 45°C. From Figure 4-4, there is not much fluctuation trend in pure water interaction. The trend rapidly damped, showing the gradual smearing out of short-range order of water.

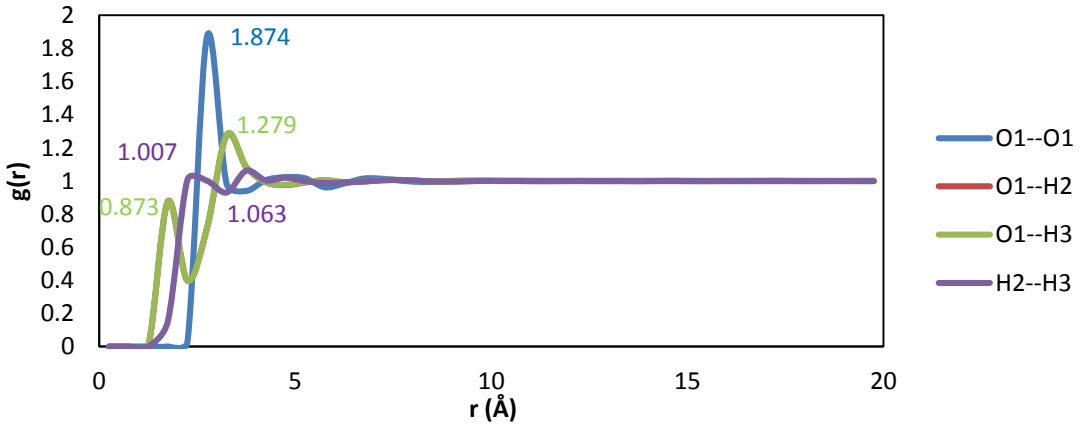

Figure 4-4: Molecule interaction in pure H_2O molecules at 45°C

Figure 4-4 and Figure 4-5 show that the trend of molecular interaction for H_2O is almost the same for both temperature of 40 ℃ and 45 ℃. The line O1—H2 interaction has the same Angstrom value and function g(r) with O1—H3 for both temperature of 40°C and 45°C.

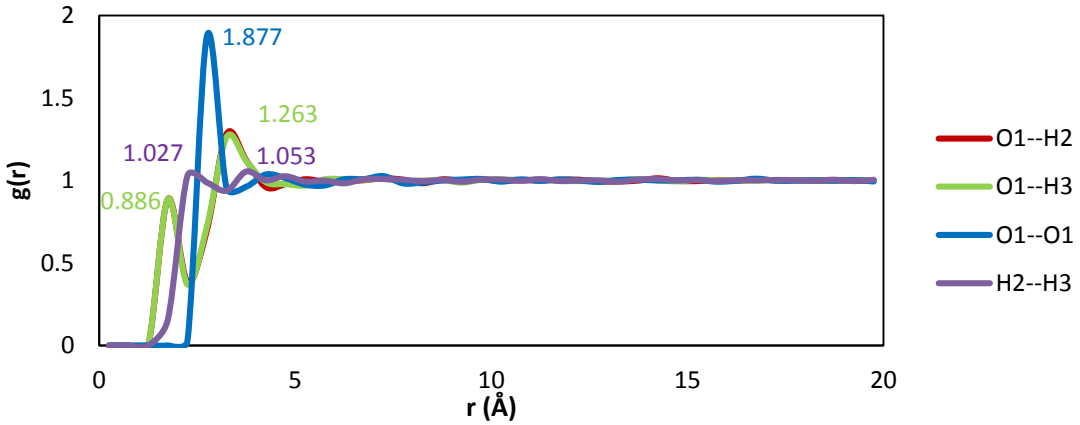

Figure 4-5: Molecule interaction in pure H_2O molecules at 40°C

For Table 4-3 and Table 4-4, the interaction of O1—O1 has the highest peak but the interaction of H2—H3 has the lowest peak. The electronegativity of oxygen atom is higher than the electronegativity of hydrogen atom. Therefore, two oxygen atoms with higher electronegativity create higher repulsive force as compared to two hydrogen atoms with lower electronegativity. The line O1—H2 interaction has the same Angstrom value and function g(r) with O1—H3 for both temperature of 40°C and 45°C. Hence, the effect of temperature on the interaction is not significant for H_2O. The trend of molecular interaction for H_2O at 40°C as shown in Figure 4-5 is similar with 45°C. The temperature range used in this study keep the water remain in liquid phase and results similar pattern observed in this study. The trend rapidly damped, showing the gradual smearing out of short-range order of water.

Table 4-3: Data of function g(r) peak for different atoms' interaction of pure H_2O at 45 ℃

Type of interactions	First peak	Highest peak
O1—O1	1.874	1.874
O1—H2	0.873	1.279
O1—H3	0.873	1.279
H2—H3	1.007	1.063

Table 4-4: Data of function g(r) peak for different atoms' interaction of pure H_2O at 40 ℃

Type of interactions	First peak	Highest peak
O1—O1	1.877	1.877
O1—H2	0.886	1.263
O1—H3	0.886	1.263
H2—H3	1.027	1.053

4.1.1.2 Methyldiethanolamine (MDEA)

The interaction between methyldiethanolamine (MDEA) molecules are analysed in the temperature of 45 ℃. Figure 4-6 shows the molecular interactions between MDEA molecules. It is seen that the –OH groups between MDEA molecules contribute the higher interaction compared to the interaction between –OH group and –N group. It is due to the polar bond between –OH groups of MDEA.

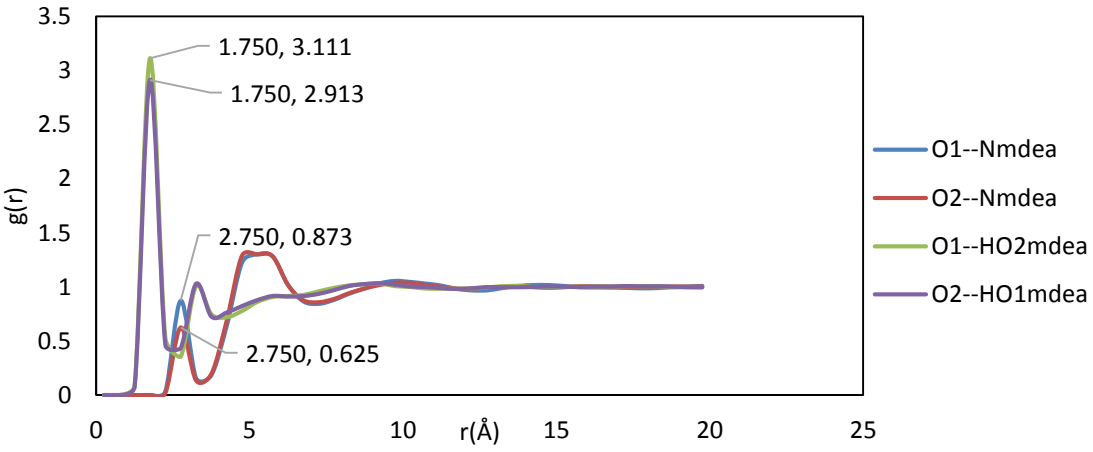

Figure 4-6: Molecule interaction in pure MDEA molecules at 45 ℃

The data of the interaction for Figure 4-6 can be summarized into the following table.

Table 4-5: Data of function g(r) peak for atoms' interaction of pure MDEA at 45°C

Type of interactions	First peak	Highest peak
O1—N_{MDEA}	2.75	0.873
O2—N_{MDEA}	2.75	0.625
O1—$HO2_{MDEA}$	1.75	3.111
O2—$HO1_{MDEA}$	1.75	2.913

However, in primary system, the interaction between same molecules cannot bring any obvious effect on the absorption process because the data is so close to each other for the respective trends (O–HO_{MDEA} and O–N_{MDEA}). It can only be concluded that the interaction between same molecules provides more understanding on intramolecular force. Hence, it does not give insight on how the absorption process will occur because absorption process should include intramolecular and intermolecular force of interaction. So, a further stage of binary system and tertiary system is carried out to a more details of interaction between molecules.

4.1.2 Binary system (MDEA+H_2O)

The interaction of nitrogen and oxygen atoms in MDEA and hydrogen atom in H_2O is analysed through characterization of radial distribution function (RDF) as shown in Figure 4-7. The results show two kinds of interaction based on amino group, –N and hydroxyl group, –OH of MDEA with water molecule. It is clearly seen that the –OH group of MDEA achieves higher interaction with g(r) = 1.103 compared to the –N group of MDEA with H_2O which has g(r) = 0.762. It can be concluded that H_2O has stronger intermolecular force of polar bond with –OH group of MDEA compared with –N group of MDEA since the electronegativity for oxygen atom is bigger than nitrogen atom.

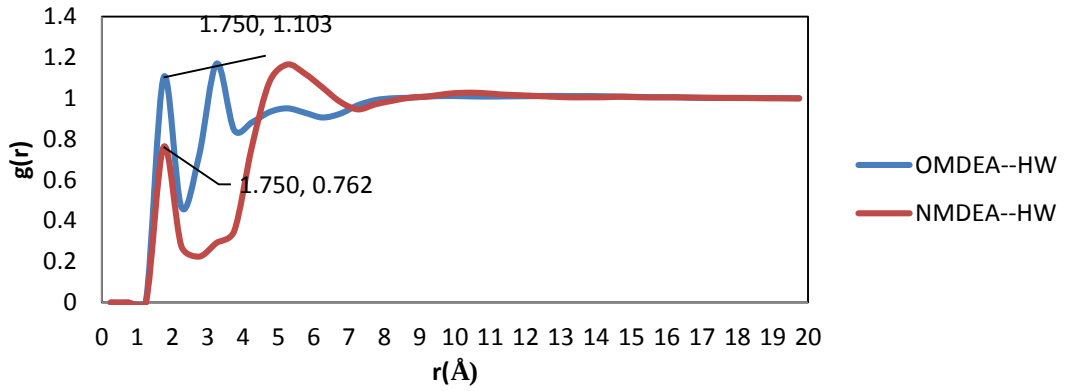

Figure 4-7: Molecular interaction in binary system (MDEA + H_2O) at 45 ℃

In the graph of RDF, peak represents the electron shell of the molecules for example first and second peak together represents the first inner electron shell of the molecules. The value of g(r) can be explained as the probability of having interaction for the molecules when there is an interaction for the molecules, it means that the adjacent atoms from molecules can be found in the inner electron shell (Farmahini, 2010). From Figure 4-7, the probability of having interaction for –OH group of reaction between MDEA and H_2O is higher than the –N group of reaction between MDEA and H_2O.

For binary system, the studies focus on the hydrogen bonding of water and –OH group of MDEA since it is proved that the –N group of MDEA has weaker interaction of hydrogen bonding with water for both temperature since it has lower value of g(r) compared to the hydrogen bonding of water and –OH group of MDEA. By analysis of Figure 4-7 (45°C) and Figure 4-8 (40°C), stronger interaction is observed at 45°C compared to 40 ℃. The g(r) value for hydrogen bonding is 1.089 and 1.103 with respect to temperature of 40ºC and 45ºC. The binary system's data acts as a reference and interpretation for tertiary system.

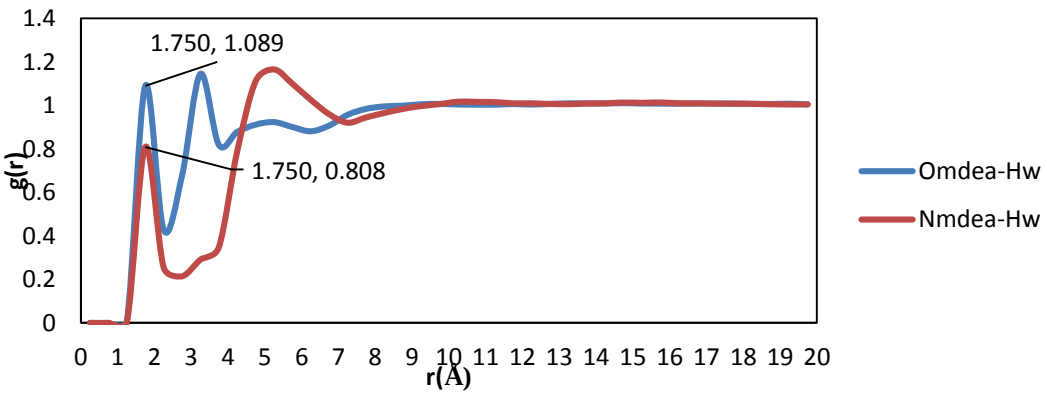

Figure 4-8: Molecular interaction in binary system (MDEA + H2O) at 40 ℃

As summary, the data collected from Figure 4-7 and Figure 4-8 is tabulated into a table as below.

Table 4-6: Data of function g(r) peak for different atoms' interaction of binary system at 40 ℃ and 45 ℃.

Temperature (°C)	N_{MDEA}-H_{H2O}		O_{MDEA}-H_{H2O}	
	r(Å)	g(r)	r(Å)	g(r)
40	1.75	0.808	1.75	1.089
45	1.75	0.762	1.75	1.103

4.1.3 Tertiary system ($MDEA+H_2O+CO_2$)

From Figure 4-9, it shows that the interaction between MDEA and H_2O occurs based on amino group, –N and hydroxyl group, –OH of MDEA. At the distance of r = 1.75Å, the molecular interaction between –OH group of MDEA and –OH group of H_2O has the highest peak of g(r) = 2.585. N_{MDEA}-O_{H2O} (blue line) interacts at a longer distance of r = 2.75 and the g(r) also has lower peak which is only 0.817. The first peak of HO_{MDEA}-O_{H2O} is higher than N_{MDEA}-O_{H2O} due to the factor of electronegativity. Higher electronegativity of oxygen atom can form a stronger intermolecular force of polar bond compared to nitrogen atom when it interacts with water.

Since HO_{MDEA}-O_{H2O} has the higher first peak compared to N_{MDEA}-O_{H2O}, it shows that the probability of HO_{MDEA}-O_{H2O} having interaction with the first neighbouring atom is higher than N_{MDEA}-O_{H2O}. Apart from that, the adjacent atoms (oxygen atom and hydrogen atom) from molecules can be found in the first inner electron shell. Therefore, the interaction between –HO group of MDEA and H_2O is stronger than the interaction between –N group of MDEA and H_2O.

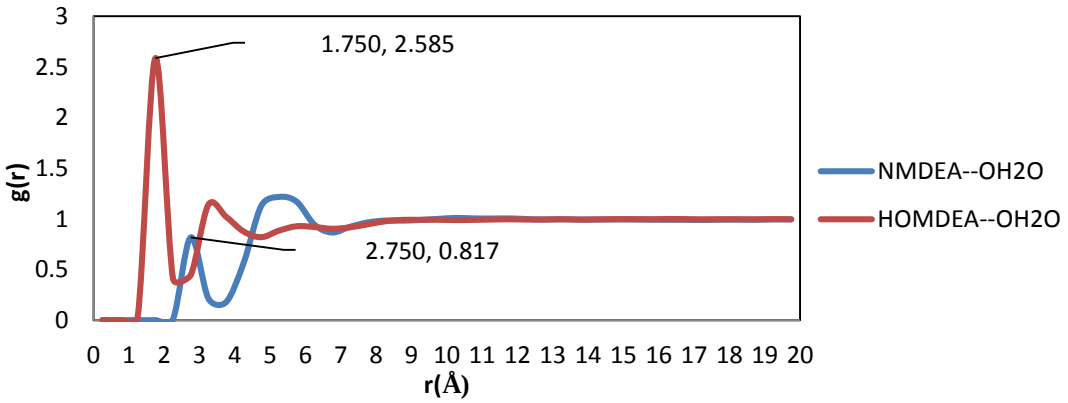

Figure 4-9: Molecular interaction between MDEA and H_2O in tertiary system at 45 ℃

Figure 4-10 shows that the CO_2 has higher interaction with –N group of MDEA compared to –OH group of MDEA. The interaction between –N group of MDEA and CO_2 has a radial distribution function of g(r) = 1.744 with distance of r = 5.25 but the interaction between –OH of MDEA and CO_2 has only radial distribution function of g(r) = 1.033 with distance of r = 5.25. The value of g(r) for the interaction between –N group of MDEA and CO_2 is much higher than the interaction between –OH of MDEA and CO_2.

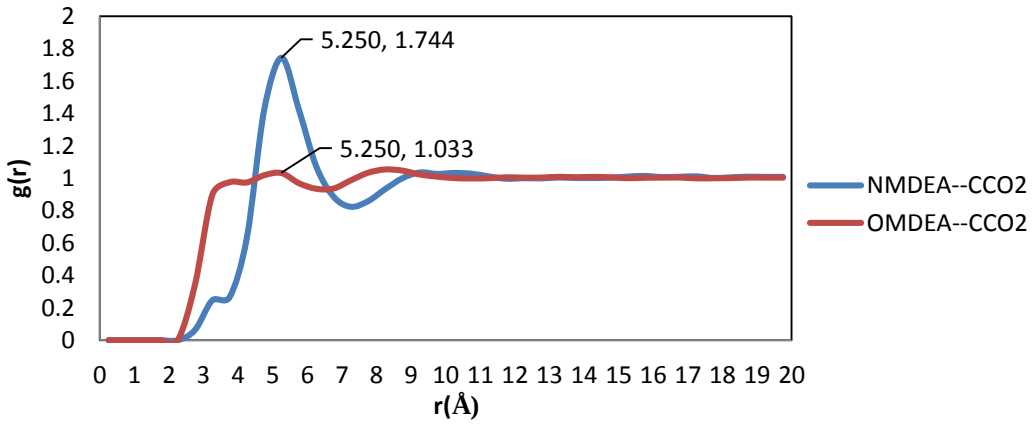

Figure 4-10: Molecular interaction between MDEA and CO_2 in tertiary system at 45℃

By referring Figure 4-9 and Figure 4-11, the g(r) values of OH_{MDEA}-O_{H2O} (red line) for tertiary system are 2.585 and 2.448 at temperature of 45℃ and 40℃ respectively. Since MDEA molecule has two hydroxyl group and one amino group, the probability to find the first neighbour atom of hydrogen bond (OH_{MDEA}-O_{H2O}) in tertiary system is higher compared to binary system. Hydrogen atom has significant influence in solubility of MDEA in water and affects the CO_2 absorption reaction in aqueous MDEA solution. When MDEA dissolves in water, it will form quaternary amine salts since MDEA is tertiary amine compound. It is observed that the intermolecular interaction strength of OH_{MDEA}-O_{H2O} is increased as the temperature increased. The similar behaviour is observed for binary system.

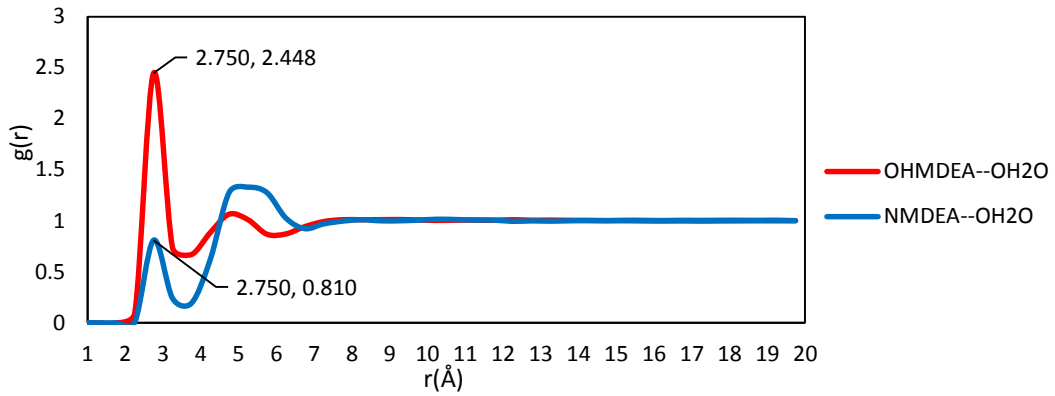

Figure 4-11: Molecular interaction between MDEA and H_2O in tertiary system at 40 ℃

As depicted in Figure 4-10 and Figure 4-12, it is known that the g(r) value of N_{MDEA}-C_{CO2} for tertiary system is 1.744 and 1.689 with respect to temperature at 45 ℃ and 40 ℃. These two figures show a higher intensity of interaction between CO_2 and amino group of MDEA.

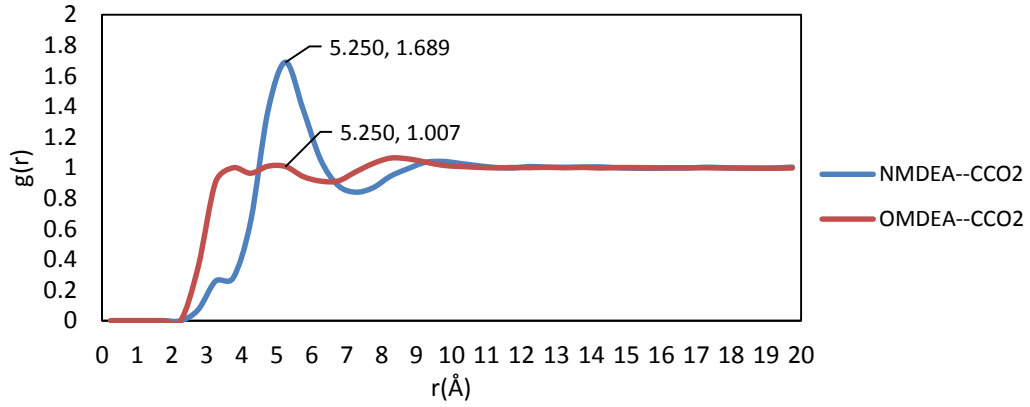

Figure 4-12: Molecular interaction between MDEA and CO_2 in tertiary system at 40 ℃

As a summary, the data collected from tertiary system which included Figure 4-9, Figure 4-10, Figure 4-11, and Figure 4-12. The data can be interpreted into Table 4-7 as below.

Table 4-7: RDF of tertiary system at 40 ℃ and 45 ℃

Temperature (^oC)	N_{MDEA}-O_{H2O}		HO_{MDEA}-O_{H2O}	
	r(Å)	g(r)	r(Å)	g(r)
40	2.750	0.810	2.750	2.448
45	2.750	0.817	1.75	2.585
	N_{MDEA}-C_{CO2}		HO_{MDEA}-C_{CO2}	
40	5.250	1.689	5.250	1.007
45	5.250	1.744	5.250	1.033

4.2 Mean square displacement

The motion of an individual molecule in a dense fluid does not follow a simple path. As it travels, the molecule is jostled by collisions with other molecules which prevent it from following a straight line. This relationship can be written as $<r^2> = 6Dt + C$.

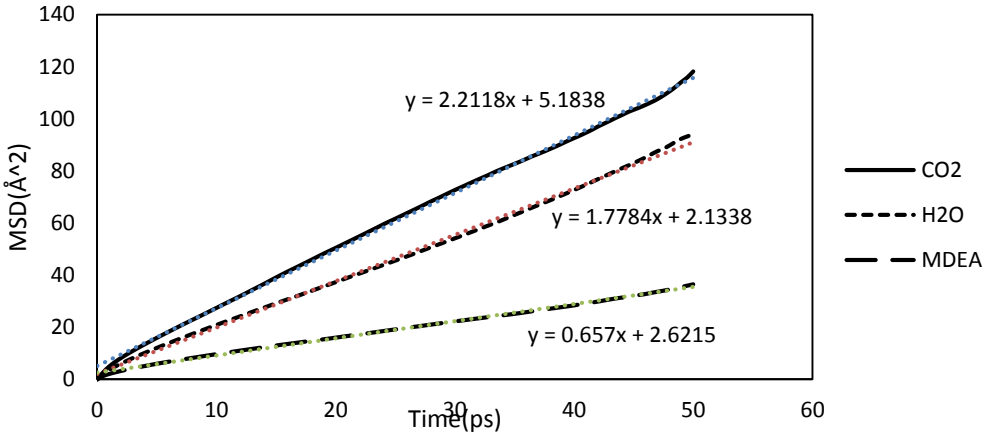

Figure 4-13: MSD graph at 40°C

The linear (straight line) dependence of the MSD plot is apparent. If the slope of this plot is taken, the diffusion coefficient, D may be readily obtained.

From Figure 4-13 and Figure 4-14, the plot is not linear at very short time. This is because the path a molecule takes will be an approximate straight line until it collides with its neighbour. Only when it starts the collision process will its path start to resemble a random walk. Until it makes that first collision, it moves with approximately constant velocity, which means the distance it travels is proportional to time, and its MSD is therefore proportional to the time squared. Thus at very short time, the MSD resembles a parabola. This is of course a simplification - the collision between molecules is not like the collision between two pebbles, it is not instantaneous in space or time, but is `spread out' a little in both. This means that the behaviour of the MSD at short time is sometimes more complicated than this MSD plot shows.

Figure 4-13 and Figure 4-14 show that the diffusion coefficient (slope) of CO_2 is much higher than the diffusion coefficient of MDEA. It means that the diffusion coefficient of CO_2 in water is higher than MDEA because the molecules of CO_2 is smaller compared to MDEA and it is in gas phase.

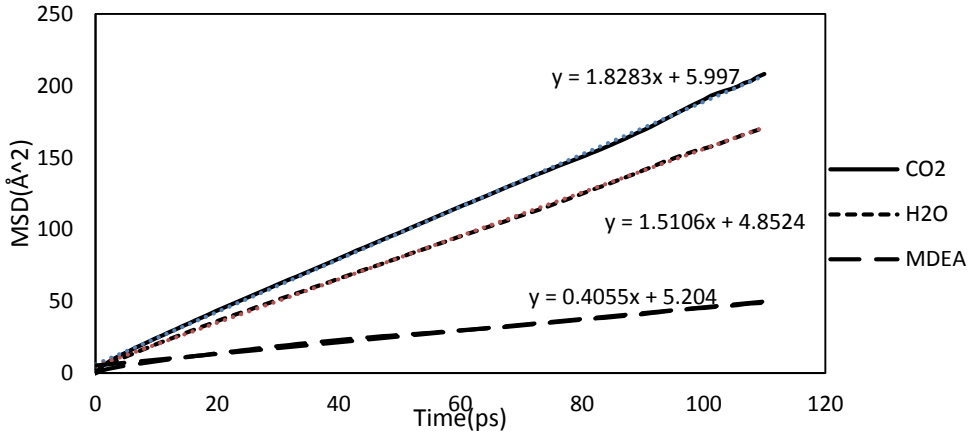

Figure 4-14: MSD graph at 45 ℃

From Figure 4-13 and Figure 4-14, gradient of each line represent the diffusion coefficient of each molecule. Hence, the diffusion coefficient and of each molecule at different temperature is shown in Table 4-8. Since MSD is equal to six times of diffusion coefficient as shown in Equation 2-23 with proper unit conversion the MSD of each molecule at different temperature can be concluded as in Table 4-8.

Table 4-8: Diffusion coefficient and MSD of each molecule at difference temperature

Molecule	Temperature (℃)			
	MSD/t (Å²/ps)		D (m²/s)	
	40	45	40	45
CO_2	2.2118	1.8283	3.686E-09	3.047E-09
H_2O	1.7784	1.5106	2.964E-09	2.518E-09
MDEA	0.6570	0.4055	1.095E-09	6.758E-10

Table 4-8 shows that the diffusion coefficient for CO_2 are the largest followed by H_2O and MDEA. CO_2 can diffuse faster due to its smaller size compared to water and MDEA molecules.

5 CONCLUSION

5.1 Conclusion

The study of intermolecular interaction in methyldiethanolamine (MDEA) absorption process for carbon dioxide capture via molecular dynamic simulation technique is performed at temperature of 40°C and 45°C. The results show that the physical interaction between CO_2, MDEA and water molecule is increased as temperature is increased. CO_2 has stronger interaction with –N group of MDEA compared to –OH group of MDEA due to the existence of hydrogen bonding with –OH group of MDEA and water molecules. Hydrogen bond is found to have significant influence on the solubility of MDEA in water and affects the CO_2 absorption reaction in aqueous MDEA solution.

The interaction of –N group of MDEA molecule with CO_2 is the initial step for the chemical reaction to occur during the absorption process to form bicarbamate ions. H_2O is more attractive with –OH group of MDEA to form a hydrogen bonding which will increase the solubility of MDEA in water. However, this study concerns the interactions occur before absorption of carbon dioxide.

In the aspect of molecular diffusion, a study on Mean Square Displacement (MSD) is carried out. It is found that the size of molecule can influence the diffusion coefficient of each molecule. The smaller size of the molecule results to the larger value of diffusion coefficient. Moreover, the phase of the molecule while occurring diffusion brings effect to the diffusion coefficient too.

5.2 Future work

Future work for this research should be carried out at a longer simulations time (longer than 5 nanoseconds) in order to get a better results. A longer simulation time calculates the intermolecular interaction between molecules and behaviour of the molecules more comprehensively.

Besides, the molecular modelling part of this study should be extended. Current study only employed temperature effects on intermolecular interaction before absorption of CO_2 occur. Other ionic species of the reaction during absorption should be included.

This is especially relevant if various thermodynamic conditions or different CO_2 loading factors are going to apply in further simulations. This is because different thermodynamic conditions can change the reaction rate and consequently lead to variation of molecular concentration (Farmahini, 2010).

In addition, hydrogen bond evaluation can be carried out by using alternative technique such as energetic definition hydrogen bonding rather than geometrical definition which is used in this study. Investigation of hydrogen bond based on energetic definition provides useful information about dynamics of hydrogen bonds by calculating pair interaction energy between molecules by means of MD simulations (Chowdhuri & Chandra, 2002).

REFERENCES

Abass A., O. (2010). CO_2 capture and separation technologies for end-of-pipe applications – A review. *Energy, 35(*6), 2610-2628.

Adam, F., Siti Hana, A. B., Mashitah, M. Y., & Tajuddin, S. N. (2013). Molecular Dynamic Simulation of the Patchouli Oil Extraction Process. *Journal pf Chemical & Engineering Data*.

Allen, M.P. & Tildesey, D. J. (1987). *Computer simulation of liquids*. New York: Oxford University Press.

A.K. Rappe ´& C.J. Casewit (1997). Molecular Mechanics Across Chemistry, University Science Books, Sausalito, CA.

Anslyn, E.V. & Dougherty, D.A. (2006). *Modern physical organic chemistry*. USA: University Science Books.

Atkins, P. W. & R. S. Friedman (2005). *Molecular Quantum Mechanics*. New York, Oxford University Press.

Balbuena, P., & Seminario, J. M. (1999). *Molecular Dynamics.* Amsterdam: Elsevier.

Barret, J.L. & Hansen, J.P. (2003). *Basic concepts for simple and complex liquids.* United Kingdom: Cambridge University Press.

Belonoshko, A. (1998). Melting of corundum using conventional and two-phase molecular dynamic simulation method. *Physics And Chemistry Of Minerals*, 25 (2), pp. 138-141.

Berendsen, H.J.C., van Gunsteren, W.F., Egberts, E. & de Vlieg, J. (1987). *Supercomputer research in chemistry and chemical engineering, chapter 7: dynamic simulation of complex molecular systems*. Minenesto: American Chemical Society. doi: 10.1021/bk-1987 0353.ch007

Born, M., & Huang, K. (1954). *Dynamical Theory of Crystal Lattices (1st ed.).* Oxford: Clarendon Press.

Chaffee, A. L., Knowles, G. P., Liang, Z., Zhang, J., Xiao, P., & Webley, P. A. (2007). CO_2 capture by adsorption: Materials and process development. *International Journal of Greenhouse Gas Control*, 1(1), 11-18.

Chakravarti S., Gupta A., & Hunek C. (2001). *Advanced Technology for the Capture of Carbon Dioxide from Flue Gases*. First National Conference on Carbon Sequestration, 2001.

Chester & Marvin (1987) *Primer of Quantum Mechanics*. John Wiley.

Chowdhuri, S. and A. Chandra (2002). "Hydrogen bonds in aqueous electrolyte solutions: Statistics and dynamics based on both geometric and energetic criteria." Physical Review E **66(**4): 041203.

Cramer, C. J. (2004). *Essentials of Computational Chemistry: Theories and Models*. West Sussex, John Wiley & Sons Ltd.

Davidson, R.M., (2007). Post-combustion Carbon Capture from Coal Fired Plants – Solvent Scrubbing. IEA Clean Coal Centre, CCC/125.

Donaldson T.L. & Nguyen Y.N. (1980). *Carbon dioxide reaction and transport into aqueous amine membranes*. Ind. Eng. Chem. Fundam., 19, pp. 260-266.

Dow. (2014). Alkyl Alkanolamines. [online] Retrieved from: http://www.dow.com/amines/prod/alkylalk.htm [Accessed: 15 Mar 2014].

Drage, T. C., Smith, K. M., Pevida, C., Arenillas, A., & Snape, C. E. (2009). Development of adsorbent technologies for post-combustion CO2 capture. *Energy Procedia,* 1(1), 881-884.

Ebbing, D.D. and Gammon, S.D. (2009). *General chemistry enhanced edition.* 9th Ed. Belmont: Brooks/Cole, Cengage Learning.

Farmahini, A. H. (2010). *Molecular dynamics simulation studies of piperazine activated MDEA absorption solution with methane and carbon dioxide*. The University of Bergen.

Furio, E. (1997). *Mean Square Displacement.* Italy.

Field, M. J. (2007). *A Practical Introduction to the Simulation of Molecular Systems*. New York, CAMBRIDGE UNIVERSITY PRESS.

Frenkel, D. & Smit, B, (2002*). Understanding molecular dynamic simulation: from algorithm to applications*. California: Academic Press.

Grande, C. A., Ribeiro, R. P. L., Oliveira, E. L. G., & Rodrigues, A. E. (2009). Electric swing adsorption as emerging CO2 capture technique. *Energy Procedia, 1(*1), 1219-1225.

Gunaratne, A. (2006). *A penalty function method for constrained molecular dynamics.* Phd thesis. Iowa State University. USA.

Gunsteren, V. W. F., W. F., R. Burgi, C. Peter, & X. Daura. 2001. *The key to solving the protein-folding problem lies in an accurate description of the denatured state.* Angew. Chem. Int. Ed. Engl. **40:**352–355

Günther, M., Maus, M., Wagner, K. G., & Schmidt, P. C. (2005). Hydrophilic solutes in modified carbon dioxide extraction-prediction of the extractability using molecular dynamic simulation. *European journal of pharmaceutical sciences :*

official journal of the European Federation for Pharmaceutical Sciences, 25(2-3), 321–9. doi:10.1016/j.ejps.2005.03.007

Hafemeidter, D., & Zahrt, J. (2004). Exchange-Charge-Model Calculation of the Born—Mayer Repulsive Potential in Ionic Gases and Crystals. *The Journal Of Chemical Physics*, 1428-1437.

Hehre, W.J. (2003). *A guide to molecular mechanics and quantum chemical calculations*. California : Wavefunction, Inc.

Hill, T.L. (1960). *An introduction to statistical thermodynamics.* New York: Dover Publication, Inc.

Hinchliffe, A. (2000). *Modelling molecular structures*. New York: John Wiley.

Hinchliffe, A. (2008). *Molecular Modelling for Beginners*. Chippenham, Wiltshire.

IEA org. (2013). CO_2 emissions from fuel combustion highlight. 2013 ed. [report] Warsaw, Poland: Maria Van der Hoeven, pp. 8 and 11.

IPCC. (2005). *IPCC special report on carbon dioxide capture and storage.* New York, Cambridge University Press.

Israelachvili, J. (2011). *Intermolecular and surface forces (3st ed.).* Amsterdam: Elsevier Academic.

Jang, S. (2007). *Molecular dynamics simulations of plastic deformation in nanocrystalline metal and alloy.* Phd thesis.

Jensen, B. (2009). *Modeling Trapping Mechanism for PCB Adsorption on Activated Carbon.* Department of Physics and Technology. Bergen, University of Bergen (UiB). Master of Science: 121.

Jensen, F. (2006). *Introduction to Computational Chemistry*. West Sussex, John Wiley & Sons Ltd.

Jensen, K. P. & W. L. Jorgensen (2006). "Halide, Ammonium, and Alkali Metal Ion Parameters for Modeling Aqueous Solutions." *Journal of Chemical Theory and Computation* **2(**6): 1499-1509.

Keffer, D. J., Baig, C., Edwards, B. & Adhangale, P. (2005). *A hamiltonian-based algorithm for rigorous molecular dynamics simulation in the NVE NVT, NPT, and NPH ensembles.*

Kierzkowska-Pawlak, H. & Chacuk, A. (2010). Kinetics of carbon dioxide absorption into aqueous MDEA solutions. Ecol. Chem. Eng. S, 17 pp. 463-475.

Kohl A.L. & Nielsen R. (1997): *Gas Purification, 5th ed*. Gulf Publishing, Houston

Laffans Petrochemical. (2007). Methyl Diethanolamine (MDEA). [online] Retrieved from: http://www.laffanspetrochemical.com/mdea.htm [Accessed: 17 March 2014].

Leach, A. R. (1996). *Molecular Modelling: Principles and Applications*. Edinburgh, Longman.

Machida, K. (1999). *Principles of molecular mechanics*. New York : Wiley.

Maddox, R. (1982). Gas conditioning and processing. Vol. 4: gas and liquid sweetening. *Penn Well Books, Tulsa, OK*.

Matteoli, E. & Mansoori, G. A. (1995). A simple expression for radial distribution functions of pure fluids and mixtures. *The Journal of Chemical Physics*, 103 (11), pp. 4672-4677

Mulliken, R. S. (1955). "Electronic Population Analysis on LCAO[Single Bond]MO Molecular Wave Functions. I." *The Journal of Chemical Physics* **23**(10): 1833-1840.

Nathalie, J. M., Penderd, v. E., Peter , W. D., Sylvie, F., & Geert, F. V. (2012). *Kinetics of Absorption of Carbon Dioxide in Aqueous MDEA Solutions with Carbonic Anhydrase ar 298 K.*

Rai, B. (2012). *Molecular modeling for the design of novel performance chemicals and materials.* Florida: CRC Press.

Schlecht, M.F. (1998). *Molecular modeling on the pc*. New York: Wiley-VCH.

Shattuck, T.W. (2008). *Molecular mechanics tutorial introduction*. Waterville: Dolby College

Steeneveldt, R., Berger, B., & Torp, T. A. (2006). CO_2 capture and storage: Closing the Knowing–Doing gap. *Chemical Engineering Research and Design*, 84(9), pp. 739-763.

Stefan, F. (2001). *Reduced Pressure, Energy and Density.*

Thompson, J. D. (2002). "*More reliable partial atomic charges when using diffuse basis sets*." PhysChemComm **5(**18): 117–134.

U. Burkert & N.L. Allinger (1982). *Molecular Mechanics*, ACS Monograph no. 177, American Chemical Society, Washington D.C.

Wang, J. M., & Hou, T. J. (2012). Diffusion Coefficient. *Application of Molecular Dynamics Simulations in Molecular Property Prediction II*, 3505-3519.

W.I. Echt. (1997). *Chemical solvent-based processes for acid gas removal in gasification applications*. pp. 3-4

Yokoyama, T., (2003): *Japanese R&D on CO_2 Capture*. Greenhouse Gas Control Technologies, Proc. of the 6th International Conference on Greenhouse Gas Control Technologies (GHGT-6), 1-4 Oct. 2002, Kyoto, Japan, J. Gale and Y. Kaya (eds.), Elsevier Science Ltd, Oxford, UK. 13-18.

Yong, Z., Mata, V., & Rodrigues, A. E. (2002). Adsorption of carbon dioxide at high temperature—a review. *Separation and Purification Technology, 26(*2-3), 195-205.

York, W.M. (2007). *Unrestrained molecular dynamic simulations of human lysosomal glycoslasparaginase in aqueous solution: A structural study of some mutations of highly conserved mammalian residues.* Phd thesis. University of North Carolina. USA.

Zumdahl, S.S., & Decoste, D.J. (2013). *Chemical princples.* 7th. Belmont: Brooks/Cole, Cengage Learning.